Electronic Supplementary Material (ESI) for ChemComm.
This journal is © The Royal Society of Chemistry 2020

Supporting information

A bicyclic unit reversal to stabilize the 12/14-helix in mixed homochiral oligoureas

Pierre Milbeo[a], Matthieu Simon[a], Claude Didierjean[b], Emmanuel Wenger[b], Emmanuel Aubert[b], Jean Martinez[a], Muriel Amblard[a], Monique Calmès[a]*, Baptiste Legrand[a]*

[1]Institut des Biomolécules Max Mousseron, IBMM, University of Montpellier, ENSCM, CNRS, Montpellier, France

[2]Université de Lorraine, CNRS, CRM2, Nancy, France.

Table of contents

General remarks

All reagents were used as purchased from commercial suppliers without further purification. Solvents were dried and purified by conventional methods prior to use. ^{1}H or ^{13}C NMR spectra (DEPT, $^{1}H/^{13}C$ 2D-correlations) were recorded with Bruker A DRX 400 and 600 spectrometers using the solvents (CD_3OH or DMSO-d_6) as internal reference. Data are reported as follows: chemical shifts (δ) in parts per million, coupling constants (J) in hertz (Hz). The ESI mass spectra were recorded with a platform II quadrupole mass spectrometer (Micromass, Manchester, UK) fitted with an electrospray source. RP-HPLC analyses were performed with a Waters model 510 instrument with variable detector using, column A: Phenomenex® Onyx Monolithic HD-C_{18}, 2µ, (50 x 4.6 mm), flow: 3 ml/min, H_2O (0.1 % TFA)/CH_3CN (0.1 % TFA), gradient 0 % (30 s), 0→100 % (3 min), 100 % (1 min) and 100→0 % (30 s); column B: Chromolith® HighResolution RP-18, 2µ, (25 x 4.6 mm), flow: 3 ml/min, H_2O (0.1 % HCO_2H)/CH_3CN (0.1 % HCO_2H), gradient 0% (45 s), 0→100 % (2.5 min) and 100 % (1 min), 100→0 % (30 s).

The enantiopure compound N-*tert*-butyloxycarbonyl-(*S*)-1,2-diaminobicyclo[2.2.2]octane (H-(*S*)-DABO-Boc)[1] and succinimidyl carbamate derivatives of Boc-β^3-amino acids Boc-APC-OSu and Boc-APPC-OSu[2] were prepared as previously described.

Scheme S1. Synthesis of mixed oligoureas **1-4**

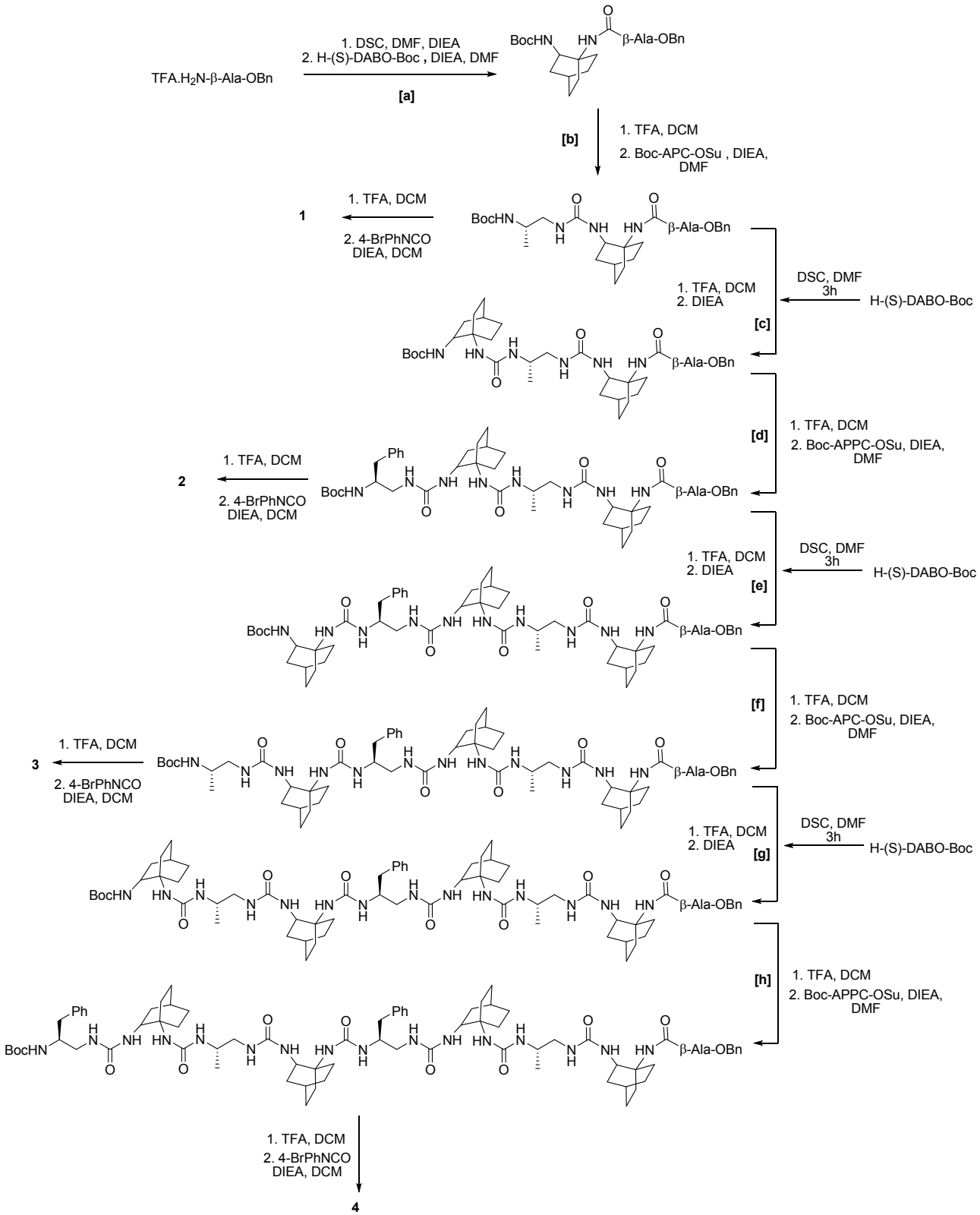

- **Procedure for the coupling [a]**:

H_2N-β-Ala-OBn, TFA (823 mg, 4.6 mmol, 1 equiv.) was dissolved in DMF (30 mL) under argon and DIEA (1.6 mL, 9.2 mmol, 2 equiv.) was added to the reaction mixture. Disuccinimidyl carbonate (DSC) (1.18 g, 4.6 mmol, 1 equiv.) was added in one portion and the reaction mixture was stirred at room temperature for 30 minutes. Activation was monitored by HPLC, column A. H-(*S*)-DABO-Boc (1.1 g, 4.6 mmol, 1 equiv.) was then added to the mixture along with DIEA (0.8 mL, 4.6 mmol, 1 equiv.), and the reaction mixture was stirred overnight at 50 °C. Once conversion was complete (monitored by HPLC), DMF was evaporated under reduced pressure and the crude was dissolved in AcOEt. The organic layer was washed with brine, $KHSO_4$ 1M (3x20 mL), $NaHCO_3$ 1M (3x20 mL) and brine, then dried over $MgSO_4$, and concentrated under reduced pressure. The obtained crude (1.98 g) was used without further purification in the next coupling. The product Boc-(*S*)-*r*BAC-β-Ala-OBn was characterized by HPLC and LC/MS. HPLC, column A (T_R 2.84 min); MS (ESI): m/z =346.2 [M-Boc+H]$^+$, 390.2 [M-*t*Bu+H]$^+$, 446.1 [M+H]$^+$.

- **Procedure for the coupling [b]**, **[d]**, **[f]** and **[h]**:

To a solution of the Boc protected growing oligomer (1 equiv.) in CH_2Cl_2 (5 mL) was added TFA (3 mL) and the reaction mixture was stirred 30 minutes at room temperature. The solvent and the TFA excess were removed under reduced pressure. The obtained crude TFA salt was dissolved in DMF (7 mL/mmol) under argon and neutralized with DIEA (3 equiv.). Compound Boc-APC-OSu (for [**b**] and [**f**]) and Boc-APPC-OSu (for [**d**] and [**h**]) (1 equiv.) was added to the reaction mixture, which was stirred overnight at room temperature. Once conversion was complete (monitored by HPLC), DMF was evaporated under reduced pressure and the crude was dissolved in AcOEt. The organic layer was washed with brine, $KHSO_4$ 1M (3x20 mL), $NaHCO_3$ 1M (3x20 mL) and brine, then dried over $MgSO_4$, and concentrated under reduced pressure. The obtained crude was used without further purification in the next coupling. The product was characterized by HPLC and LC/MS.

After coupling [**b**], starting from the crude Boc-(*S*)-*r*BAC-β-Ala-OBn (1.87 g, 4.2 mmol), the crude product (2.07 g) containing the dimer Boc-APC-(*S*)-*r*BAC-β-Ala-OBn as the major product was obtained. HPLC, column A (T_R 2.72 min); MS (ESI): m/z = 546.2 [M+H]$^+$, 568.3 [M+Na]$^+$.

After coupling [d], starting from the crude Boc-(*S*)-*r*BAC-APC-(*S*)-*r*BAC-β-Ala-OBn (0.92 g, 1.3 mmol), the crude product (1.09 g) containing the tetramer Boc-APPC-(*S*)-*r*BAC-APC-(*S*)-*r*BAC-β-Ala-OBn as the major compound was obtained. HPLC, column A (T_R 3.15 min); MS (ESI): m/z = 888.5 [M+H]$^+$, 910.5 [M+Na]$^+$.

After coupling [f], starting from the crude Boc-(*S*)-*r*BAC-APPC-(*S*)-*r*BAC-APC-(*S*)-*r*BAC-β-Ala-OBn (342 mg, 0.32 mmol), the crude product (380 mg) containing the hexamer Boc-APC-(*S*)-*r*BAC-APPC-(*S*)-*r*BAC-APC-(*S*)-*r*BAC-β-Ala-OBn as the major product was obtained. HPLC, column A (R_t 3.62 min); MS (ESI): m/z = 1154.9 [M+H]$^+$, 1176.9 [M+Na]$^+$.

After coupling [h], starting from the crude Boc-(*S*)-*r*BAC-APC-(*S*)-*r*BAC-APPC-(*S*)-*r*BAC-APC-(*S*)-*r*BAC-β-Ala-OBn (188 mg, 0.14 mmol), the crude product (177 mg) containing the octamer Boc-APPC-(*S*)-*r*BAC-APC-(*S*)-*r*BAC-APPC-(*S*)-*r*BAC-APC-(*S*)-*r*BAC-β-Ala-OBn as the major product was obtained. HPLC, column A(T_R 4.20 min); MS (ESI): m/z = 1498.1 [M+H]$^+$, 1520.0 [M+Na]$^+$.

- **Procedure for the coupling [c]**, **[e]**, and **[g]**:

To a solution of the H-(*S*)-DABO-Boc (0.5 equiv.) in DMF (4 mL/mmol) was added disuccinimidyl carbonate (DSC) (0.5 equiv.), and the reaction mixture was stirred for 3 hours (this activation step was set every 30 min with another 0.5 equiv. of H-(*S*)-DABO-Boc to provide freshly activated monomer for the coupling step)

In a different flask, the Boc-protected growing oligomer (1 equiv.) was dissolved in CH_2Cl_2 (5mL) and treated with TFA (3 mL). After 30 minutes stirring at room temperature, the solvent and TFA excess were removed under reduced pressure. The crude was then dissolved in DMF (4 mL/mmol) under argon and treated with DIEA (2 equiv.) to neutralize the TFA salt. The reaction mixture previously prepared by activation of the H-(*S*)-DABO-Boc was then added to this reaction medium and the mixture was stirred at 50 °C under argon. The conversion was monitored by HPLC and did not evolve anymore after 30 minutes. 0.5 Additional equivalent of freshly prepared activated H-(*S*)-DABO-Boc was added to the reaction mixture. The procedure was repeated until complete conversion. DMF was then evaporated under reduced pressure and the crude was purified by reverse phase flash chromatography (0 to 100% CH_3CN in water in 20 column volume). Unreacted H-(*S*)-DABO-Boc was recovered pure after purification, and fractions containing the expected oligourea as the major product gathered, concentrated and used without further purification in the next coupling. The product was characterized by HPLC and LC/MS.

After coupling [c], starting from the crude Boc-APC-(*S*)-*r*BAC-β-Ala-OBn (1.74 g, 3.2 mmol), the trimer Boc-(*S*)-*r*BAC-APC-(*S*)-*r*BAC-β-Ala-OBn (0.98 g, 1.38 mmol, 43 % yield) was obtained. HPLC, column A (T_R 3.00 min); MS (ESI): m/z = 712.5 $[M+H]^+$, 734.5 $[M+Na]^+$.

After coupling [e], starting from the crude Boc-APPC-(*S*)-*r*BAC-APC-(*S*)-*r*BAC-β-Ala-OBn (800 mg, 0.90 mmol), the pentamer Boc-(*S*)-*r*BAC-APPC-(*S*)-*r*BAC-APC-(*S*)-*r*BAC-β-Ala-OBn (342 mg, 0.32 mmol, 36 % yield) was obtained. HPLC, column A (T_R 3.59 min); MS (ESI): m/z = 1054.8 $[M+H]^+$, 1076.7 $[M+Na]^+$.

After coupling [f], starting from the crude Boc-APC-(*S*)-*r*BAC-APPC-(*S*)-*r*BAC-APC-(*S*)-*r*BAC-β-Ala-OBn (200 mg, 0.17 mmol), the heptamer Boc-(*S*)-*r*BAC-APC-(*S*)-*r*BAC-APPC-(*S*)-*r*BAC-APC-(*S*)-*r*BAC-β-Ala-OBn (188 g, 0.14 mmol, 84 % yield) was obtained. HPLC, column A (T_R 4.16 min); MS (ESI): m/z = 1321.0 $[M+H]^+$, 1343.0 $[M+Na]^+$.

- **Procedure for the synthesis of mixed oligoureas 1-4**:

To a solution of the Boc-protected dimer, tetramer, hexamer and octamer (1 equiv.) in CH_2Cl_2 (5 mL/0.1 mmol) was added TFA (3 mL/0.1 mmol), and the reaction mixture was stirred at room temperature for 30 minutes. Solvent and TFA excess were then removed under reduced pressure. The residue was dissolved in CH_2Cl_2 (2 mL/0.1 mmol) under argon and neutralized with DIEA (52 mL, 0.3 mmol, 3 equiv.). 4-bromophenylisocyanate (1 equiv.) was added to the mixture and the reaction medium was stirred at room temperature under argon for 2 hours. The reaction was then quenched with $KHSO_4$ 1 M, and the organic layer was washed with $KHSO_4$ 1 M (3x5 mL), $NaHCO_3$ 1 M (3x5 mL) and brine, dried over $MgSO_4$ and concentrated under reduced pressure. The crude was purified by chromatography on silica gel (AcOEt/Cyclohexane 1:1, then 2 to 10% MeOH in CH_2Cl_2). Pure fractions were collected, the solvent was removed under reduced pressure, and the mixed oligoureas **1-4** were obtained as white solids.

Oligourea 1 Br-C_6H_4-NH-CO-APC-(*S*)-*r*BAC-β-Ala-OBn
Synthesized according to the general procedure starting from Boc-APC-(*S*)-*r*BAC-β-Ala-OBn (150 mg, 0.27 mmol). The expected compound **1** (100 mg, 0.15 mmol, 55 % yield) was obtained as a white solid. HPLC, column B (T_R 1.84 min);MS (ESI): *m/z* = 643.1.1and 645.1 $[(M+H)^+]$; ^1H, ^{13}C and ^{15}N NMR chemical shifts for oligoureas **1** were performed in CD_3OH and DMSO-d_6 and are reported in the Supplementary Material, "NMR and molecular modelling studies" section.

Oligourea 2 Br-C_6H_4-NH-CO-APPC-(*S*)-*r*BAC-APC-(*S*)-*r*BAC-β-Ala-OBn

Synthesized according to the general procedure from Boc-APPC-(*S*)-*r*BAC-APC-(*S*)-*r*BAC-β-Ala-OBn (96 mg, 0.11 mmol). The expected pure compound **2** (57 mg, 0.06 mmol, 54 % yield) was obtained as a white solid. HPLC, column B (T_R 2.18 min);MS (ESI): *m/z* = 985.5 and 987.4 [$(M+H)^+$]; ^1H, ^{13}C and ^{15}N NMR chemical shifts for oligoureas **2** are reported in CD_3OH and DMSO-d_6 in the Supplementary Materials section, "NMR and molecular modelling studies".

Oligourea 3 Br-C_6H_4-NH-CO-APC-(*S*)-*r*BAC-APPC-(*S*)-*r*BAC-APC-(*S*)-*r*BAC-β-Ala-OBn
Synthesized according to the general procedure from Boc-APC-(*S*)-*r*BAC-APPC-(*S*)-*r*BAC-APC-(*S*)-*r*BAC-β-Ala-OBn (150 mg, 0.13 mmol). The expected pure **3** (110 mg, 0.11 mmol, 85 % yield) were obtained as a white solid. HPLC, column B (T_R 2.60 min);MS (ESI): *m/z* = 626.4 and 627.3 [$(M+2H)^{2+}$], 1251.7 and 1253.6 [$(M+H)^+$]; ^1H, ^{13}C and ^{15}N NMR chemical shifts for oligoureas **3** are reported in CD_3OH and DMSO-d_6 in the Supplementary Materials section, "NMR and molecular modelling studies".

Oligourea 4 Br-C_6H_4-NH-CO-APPC-(*S*)-*r*BAC-APC-(*S*)-*r*BAC-APPC-(*S*)-*r*BAC-APC-(*S*)-*r*BAC-β-Ala-OBn
Synthesized according to the general procedure from Boc-APPC-(*S*)-*r*BAC-APC-(*S*)-*r*BAC-APPC-(*S*)-*r*BAC-APC-(*S*)-*r*BAC-β-Ala-OBn (146 mg, 0.098 mmol). The expected pure compound **4** (90 mg, 0.056 mmol, 57 % yield) was obtained as a white solid. HPLC, column B (T_R 4.05 min); MS (ESI): *m/z* = 797.7 and 798.6 [$(M+2H)^{2+}$], 1594.2 and 1596.3 [$(M+H)^+$]; ^1H, ^{13}C and ^{15}N NMR chemical shifts for oligoureas **4** are reported in CD_3OH and DMSO-d_6 in the Supplementary Materials section, "NMR and molecular modelling studies".

- **Optimization of syntheses of the mixed oligoureas**:

We also initially considered the use of the preformed succinimidyl carbamate derivative of H-(*S*)-DABO-Boc (SuO-CO-DABO-Boc), as precursor for insertion of the cyclic residue. However, formation and isolation of this activated compound using N,N'-disuccinimidyl carbonate (DSC) as reagent resulted in a significant formation of the corresponding cyclic urea (i.e. allophanate, Fig. 1d) along with the expected product.[a] This intramolecular side reaction was minor during the previous preparation of the succinimidyl carbamate of Boc-(*S*)-BAC-OSu from Boc-(*S*)-ABOC-OH[b] whereas a large extend of a cyclic urea has been observed during the development of the DABO synthesis.[c] Moreover, attempts to activate the amine function of the terminal acyclic residue of the growing oligourea, H-(*S*)-APC-(*S*)-rBAC-β-Ala-OBn, as a possible alternative, led to the formation of the corresponding cyclic biuret (Fig. 1d). A similar result has been previously observed during the synthesis of acyclic oligoureas. Other types of activation using DCI and triphosgene reagents were also been tested and showed that the DSC reagent led to the best results. Moreover, the bi-protection of the amine function of DABO [-$N(Boc)_2$ instead of –NHBoc], that should avoid cyclic urea formation, has been investigated unsuccessfully due to the synthetic difficulties for introduction of the two Boc groups.

(a) J. Fremaux, L. Fischer, T. Arbogast, B. Kauffmann and G. Guichard, Angew. Chem. Int. Ed., 2011, **50**, 11382-11385.
(b) C. André, B. Legrand, L. Moulat, E. Wenger, C. Didierjean, E. Aubert, M. C. Averlant-Petit, J. Martinez, M. Amblard and M. Calmes, Chem. Eur. J., 2013, **19**, 16963-16971
(c) P. Milbeo, L. Moulat, C. Didierjean, E. Aubert, J. Martinez and M. Calmès, J. Org. Chem., 2017, **73**, 3144-3151

Liquid Chromatography (LC) - Mass spectrometry (MS)

Figure S1. LC/MS analysis of compound **1**

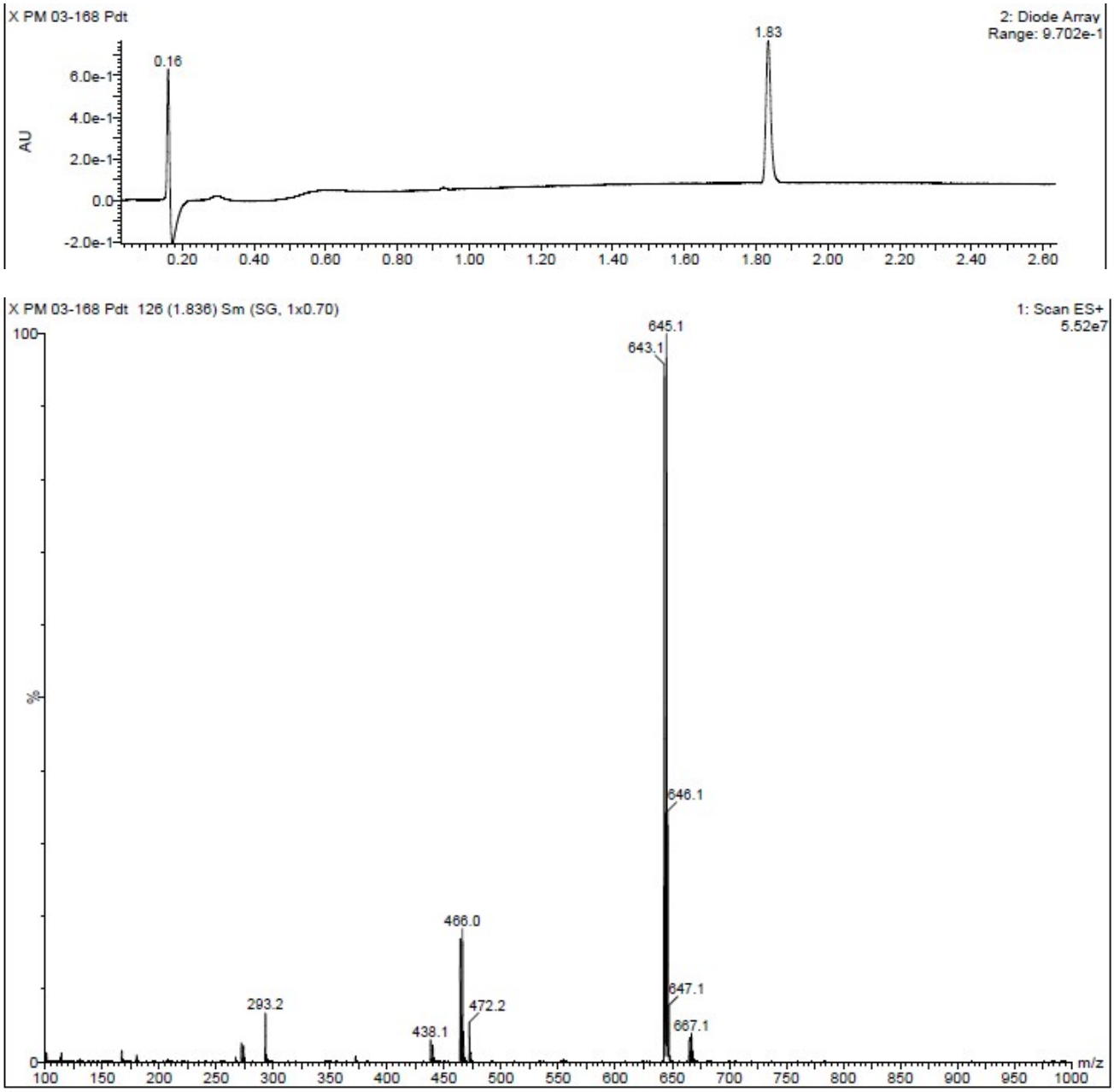

Figure S2. LC/MS analysis of compound **2**

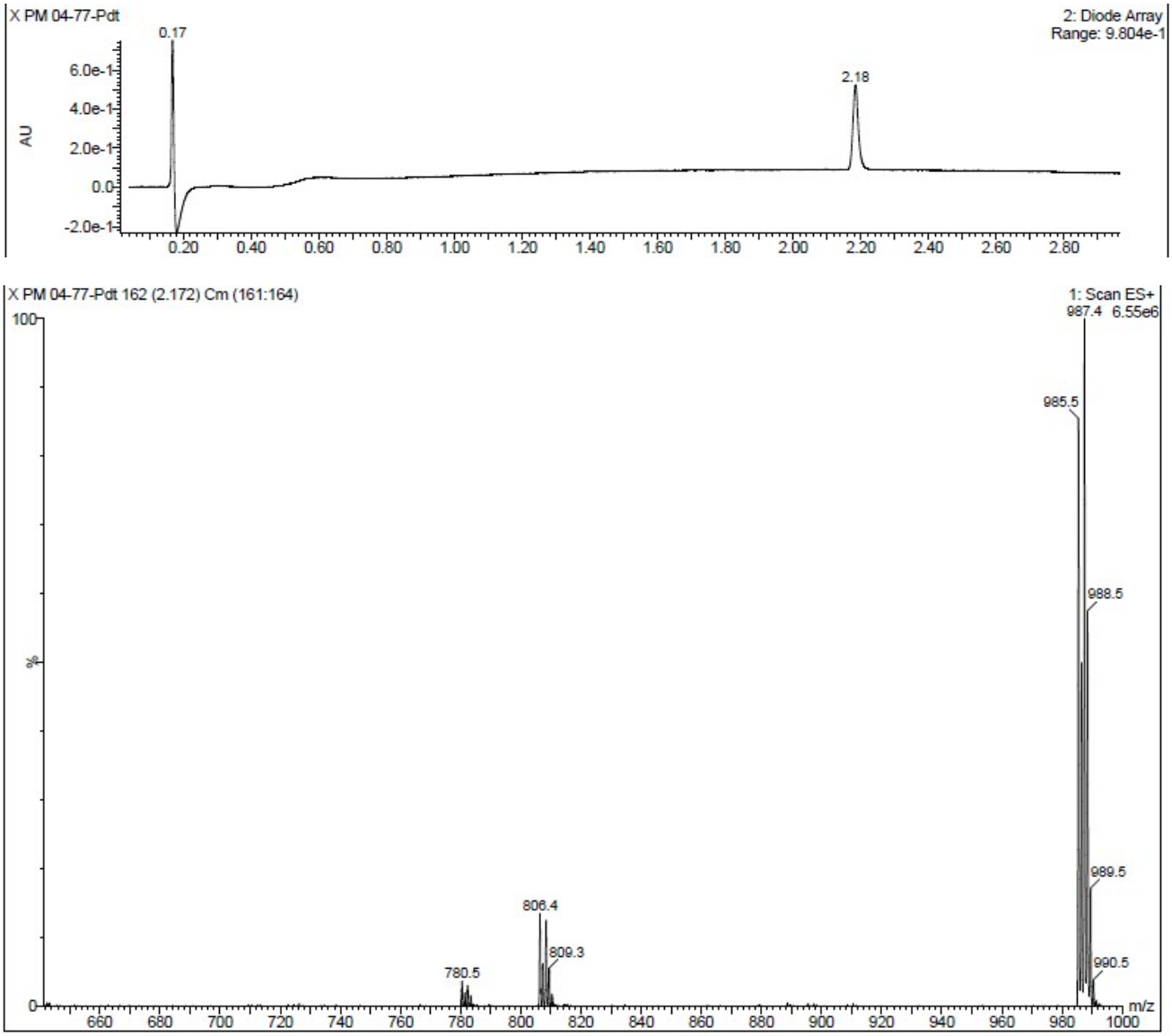

Figure S3. LC/MS analysis of compound **3**

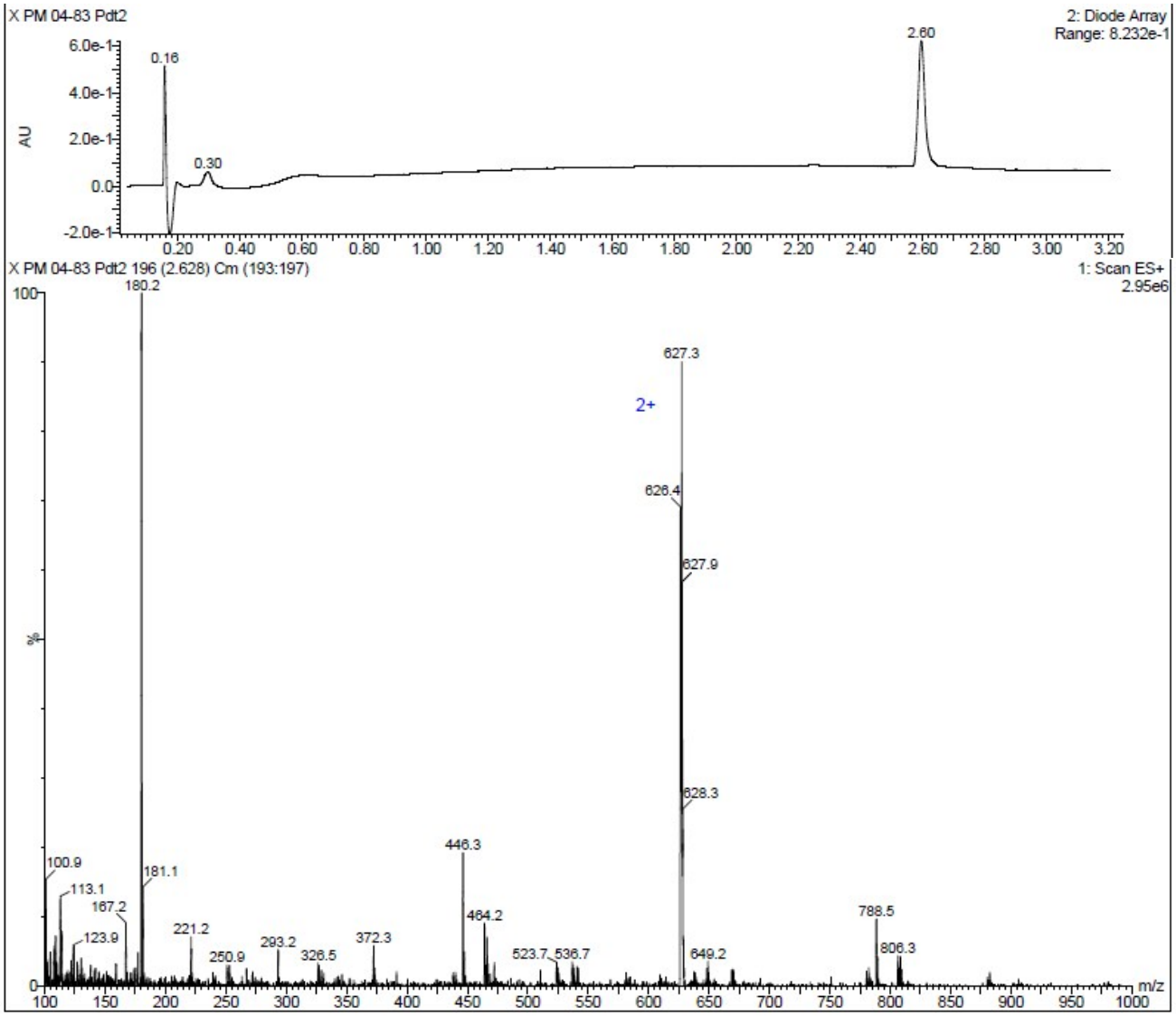

Figure S4. LC/MS analysis of compound **4**

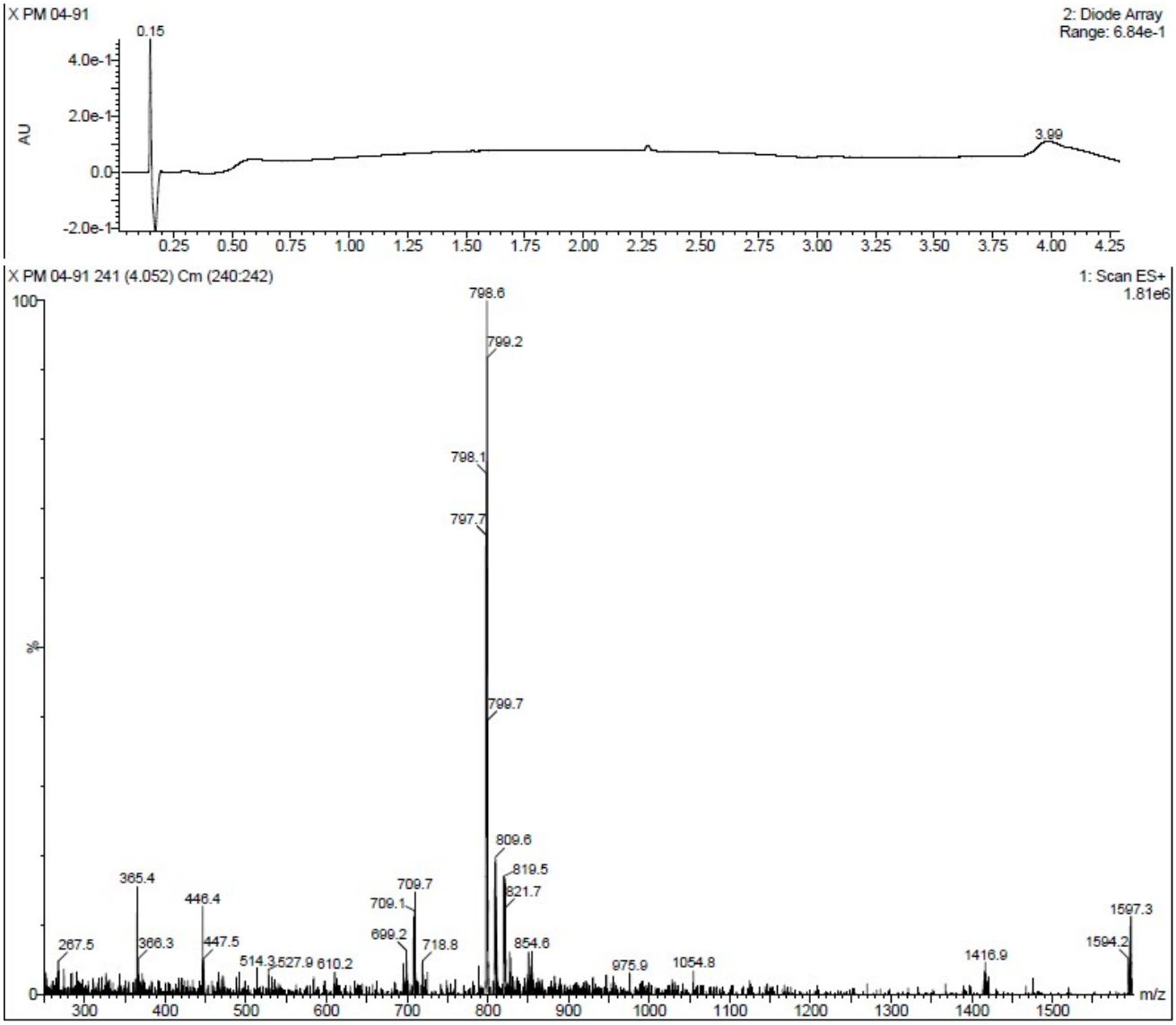

Figure S5. (*S*)-*r*BAC/(*S*)-AAC oligoureas.

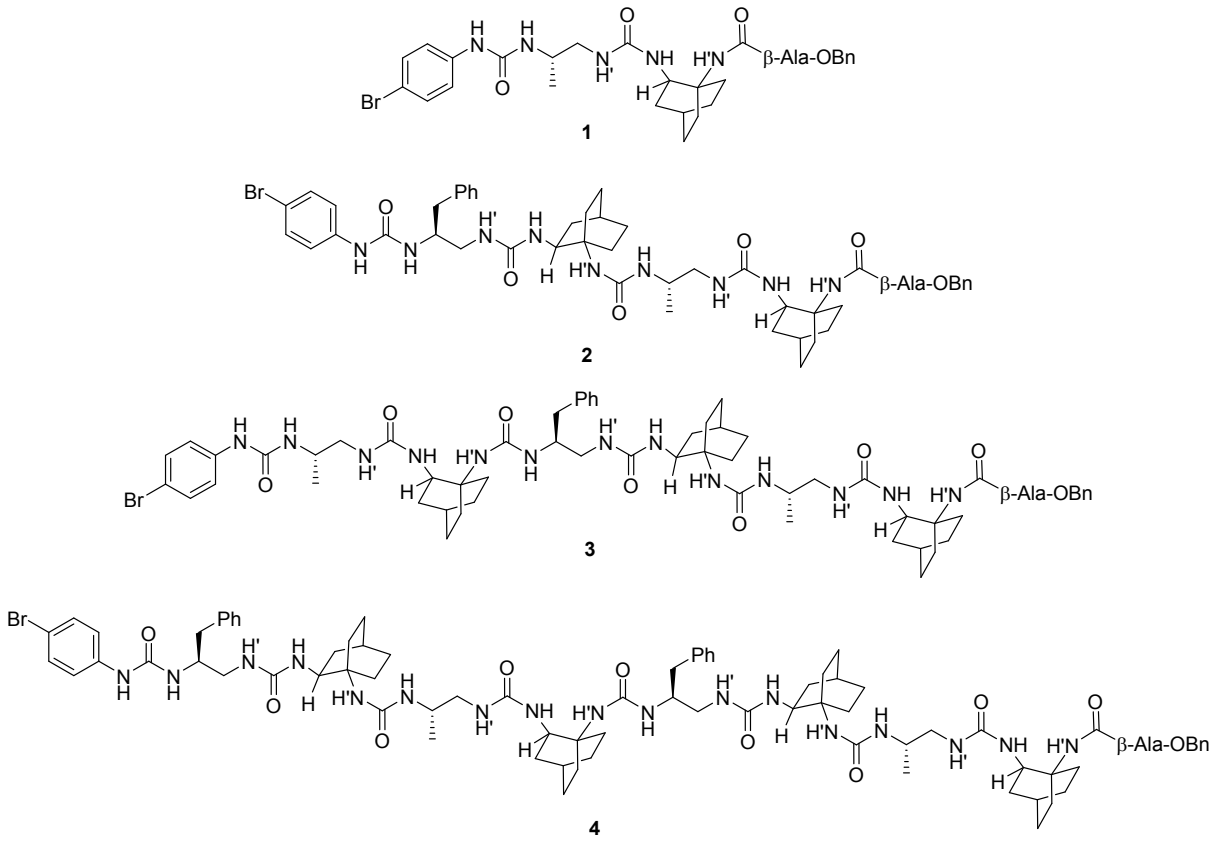

Figure S6. Nomenclature used for the various atoms of each residue.

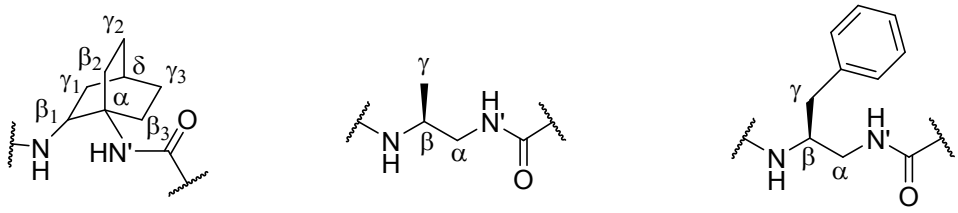

*(S)-r*BAC unit APC unit APPC unit

Circular dichroism

CD experiments were performed using a Jasco J815 spectropolarimeter. Spectra were obtained using a 1 mm path length CD cuvette, at 20–55 °C, over a wavelength range of 190–260 nm. Continuous scanning mode was used, with a response of 1.0 s with 0.2 nm steps and a bandwidth of 2 nm. The signal-to-noise ratio was improved by acquiring each spectrum over an average of three scans. The baseline was corrected by subtracting the background from the sample spectrum. Samples were dissolved in a spectrophotometric grade methanol at 100–200 μM.

Figure S7. CD spectra of dimer **1** (yellow), tetramer **2** (green), hexamer **3** (blue) and octamer **4** (purple) recorded at 20°C. CD spectra recorded at 20°C, 55°C and then back to 20°C: yellow, yellow dashed line and orange for **1**; green, green dashed line and dark green for **2**; blue, blue dashed line and dark blue for **3**; magenta, purple dashed line and purple for **4**, respectively.

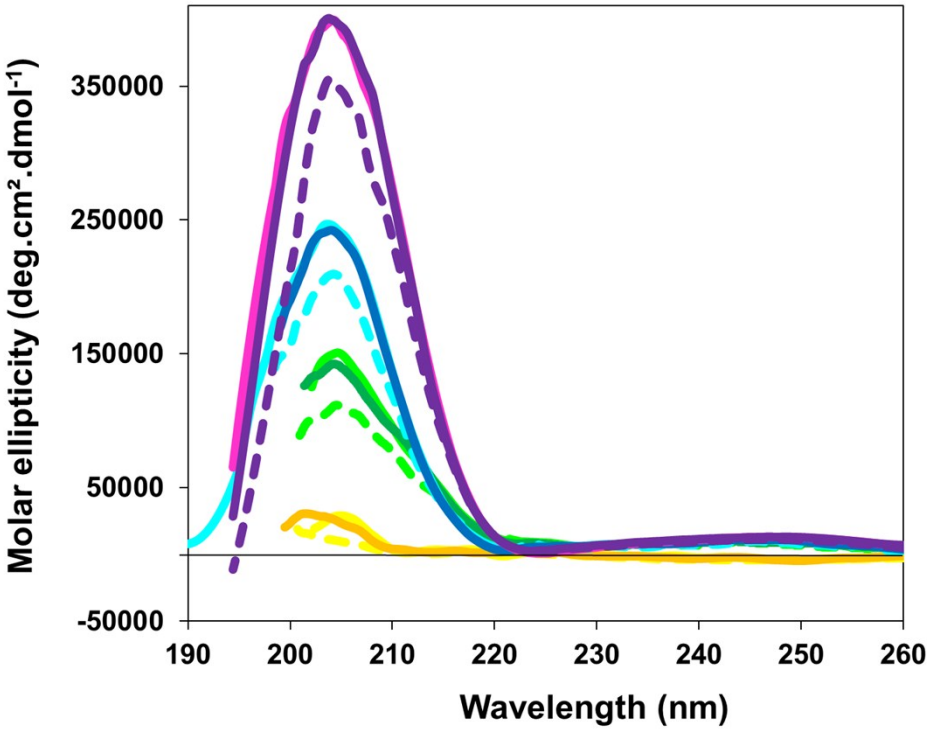

NMR and molecular modelling studies

NMR experiments. NMR samples containing 2-4 mM of oligoureas **1**, **2**, **3** and **4** were dissolved in CD_3OH or in DMSO-d_6. All spectra were recorded on a Bruker Avance 600 AVANCE III spectrometer equipped with a 5 mm triple-resonance cryoprobe (^1H, ^{13}C, ^{15}N) at the "Laboratoire de Mesures Physiques (LMP)" of the University of Montpellier (UM). Homonuclear 2D spectra DQF-COSY, TOCSY (DIPSI2) and ROESY were typically recorded in the phase-sensitive mode using the States-TPPI method as data matrices of 256-700 real (t1) × 2048 (t2) complex data points; 8-64 scans per t1 increment with 1.0-1.5 s recovery delay and spectral width of 6009 Hz in both dimensions were used. The mixing times were 60 ms for TOCSY and 450 ms for the ROESY experiments. In addition, 2D heteronuclear spectra ^{15}N- and ^{13}C-HSQC were performed (8-32 scans, 256-512 real (t1) × 2048 (t2) complex data points). Spectra were processed with Topspin (Bruker Biospin) and visualized with Topspin or NMRview[a] on a Linux station. Matrices were zero-filled to 1024 (t1) x 2048 (t2) points after apodization by shifted sine-square multiplication and linear prediction in the F1 domain. Chemical shifts were referenced to the tetramethylsilane (TMS).

Structure calculations. ^1H, ^{15}N and ^{13}C chemical shifts were assigned according to classical procedures. NOE cross-peaks were integrated and assigned within the NMRView software. The volumes of NOE peaks between methylene pair protons were used as reference of 1.8 Å. The lower bound for all restraints was fixed at 1.8 Å and upper bounds at 2.7, 3.3 and 5.0 Å, for strong, medium and weak correlations, respectively. Pseudo-atom corrections of the upper bounds were applied for unresolved aromatic, methylene and methyl proton signals as described previously.[b] Structure calculations were performed with AMBER 11[c] in two stages: cooking, simulated annealing in vacuum. The cooking stage was performed at 1000 K to generate 100 initial random structures. Simulated annealing calculations were carried during 20 ps (20000 steps, 1 fs long). First, the temperature was risen quickly and was maintained at 1000 K for the first 5000 steps, then the system was cooled gradually from 1000 K to 100 K from step 5001 to 18000 and finally the temperature was brought to 0 K during the 2000 remaining steps. For the 3000 first steps, the force constant of the distance restraints was increased gradually from 2.0 kcal.mol-1.Å to 20 kcal.mol-1.Å. For the rest of the simulation (step 3001 to 20000), the force constant was kept at 20 kcal.mol^{-1}.Å. The 15 lowest energy structures with no violations > 0.3 Å were considered representative of the compound structure. The representation and quantitative analysis were carried out using MOLMOL[d] and PyMOL (Delano Scientific).

(a) B. A. Johnson, R. A. Blevins, J. Biomol.NMR,1994, 4, 603-614
(b) K. Wüthrich, NMR of Proteins and Nucleic acids;Wiley Interscience: New York, 1986
(c) D.A. Case et al., AMBER 11, University of California, San Francisco, 2010
(d) R. Koradi, M. Billeter, K. Wuthrich, J. Mol. Graph., 1996, 14, 51-5, 29-32

Oligourea 1

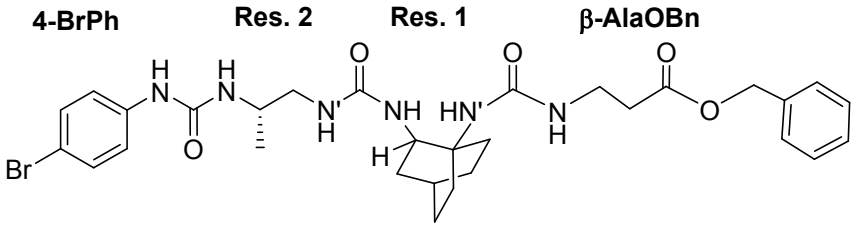

Table S1. ^{1}H NMR chemical shifts for **1** in CD_3OH at 313 K

Residue	HN	HN'	$^{\alpha}$CH	$^{\beta/\beta_1}$CH	$^{\beta_2}$CH	$^{\beta_3}$CH	$^{\gamma/\gamma_1}$CH	$^{\gamma_2}$CH	$^{\gamma_3}$CH	$^{\delta}$CH
β-Ala-OBn	5.98	-	2.45	3.28	-	-	-	-	-	-
Res. 1	6.17	5.77	-	3.91	1.60	1.72	1.31 2.14	1.63	1.54	1.54
Res. 2	5.94	6.03	3.03 3.28	3.90	-	-	1.12	-	-	-
4-BrPh	8.23	-	-	-	-	-	-	-	-	-

Table S2. ^{1}H NMR chemical shifts for **1** in DMSO-d_6 at 298 K

Residue	HN	HN'	$^{\alpha}$CH	$^{\beta/\beta_1}$CH	$^{\beta_2}$CH	$^{\beta_3}$CH	$^{\gamma/\gamma_1}$CH	$^{\gamma_2}$CH	$^{\gamma_3}$CH	$^{\delta}$CH
β-Ala-OBn	5.98	-	2.42	3.13	-	-	-		-	-
Res. 1	6.14	5.70	-	3.73	1.50 2.18	1.56 2.01	1.19 2.01	1.57	1.57	1.49
Res. 2	6.08	5.98	3.04	3.71	-	-	1.03	-	-	-
4-BrPh	8.63	-	-	-	-	-	-		-	-

Oligourea 2

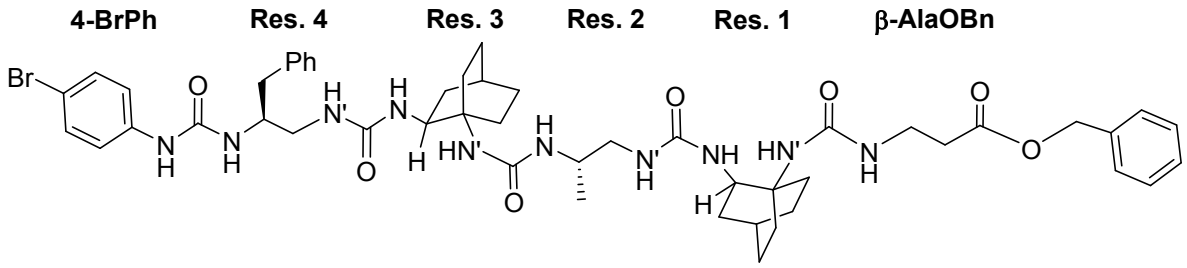

Table S3. ^{1}H NMR chemical shifts for **2** in CD_3OH at 298 K

Residue	HN	HN'	$^{\alpha}$CH	$^{\beta/\beta_1}$CH	$^{\beta_2}$CH	$^{\beta_3}$CH	$^{\gamma/\gamma_1}$CH	$^{\gamma_2}$CH	$^{\gamma_3}$CH	$^{\delta}$CH
β-Ala-OBn	6.33	-	2.54	3.28 3.37	-	-	-	-	-	-
Res. 1	6.43	5.92	-	4.04	1.46 1.57	1.71 2.53	1.34 2.17	1.60	1.60	1.60
Res. 2	5.70	6.66	2.47	3.80	-	-	0.94	-	-	-
Res. 3	6.14	5.53	-	4.34	1.63 1.90	1.93 2.31	1.31 2.10	1.60	1.60	1.60
Res. 4	6.06	6.15	3.58	4.15	-	-	2.73 2.82	-	-	-
4-BrPh	8.41	-	-	-	-	-	-	-	-	-

Table S4. ^{1}H NMR chemical shifts for **2** in DMSO-d_6 at 298 K

Residue	HN	HN'	$^{\alpha}$CH	$^{\beta/\beta_1}$CH	$^{\beta_2}$CH	$^{\beta_3}$CH	$^{\gamma/\gamma_1}$CH	$^{\gamma_2}$CH	$^{\gamma_3}$CH	$^{\delta}$CH
β-Ala-OBn	6.01	-	2.45	3.10 3.20	-	-	-	-	-	-
Res. 1	6.10	5.67	-	3.80	1.47 1.70	1.89 2.04	1.18 2.02	1.50	1.50	1.50
Res. 2	5.67	6.10	2.41 3.14	3.59	-	-	0.83	-	-	-
Res. 3	6.17	5.50	-	3.99	1.57 1.93	1.60 2.33	1.19 1.96	1.50	1.50	1.50
Res. 4	6.22	6.14	2.94 3.27	3.92	-	-	2.66 2.76	-	-	-
4-BrPh	8.70	-	-	-	-	-	-	-	-	-

Oligourea 3

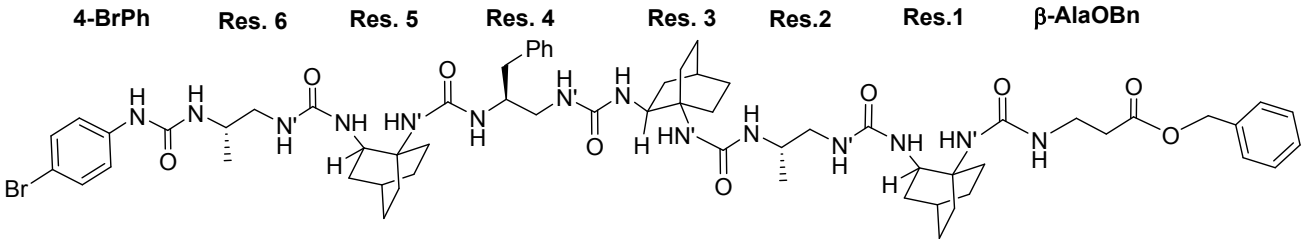

Table S5. ^{1}H NMR chemical shifts for **3** in CD_3OH at 298 K

Residue	HN	HN'	$^{\alpha}$CH	$^{\beta_1}$CH	$^{\beta_2}$CH	$^{\beta_3}$CH	$^{\gamma_1}$CH	$^{\gamma_2}$CH	$^{\gamma_3}$CH	$^{\delta}$CH
β-Ala-OBn	6.30	-	2.52	3.29 3.37	-	-	-	-	-	-
Res. 1	6.46	5.93	-	4.06	nd	nd	1.37 2.18	1.61	1.61	1.61
Res. 2	6.00	6.69	2.37 3.39	3.82	-	-	0.96	-	-	-
Res. 3	6.16	5.57	-	4.38	nd	nd	1.34 2.10	1.61	1.61	1.61
Res. 4	5.94	6.85	2.40 3.67	3.91	-	-	2.60 2.68	-	-	-
Res. 5	6.09	5.64	-	4.40	nd	nd	1.32 2.07	1.61	1.61	1.61
Res. 6	5.95	6.09	2.59 3.48	3.79	-	-	1.00	-	-	-
4-BrPh	8.34	-	-	-	-	-	-	-	-	-

Table S6. ^{1}H NMR chemical shifts for **3** in DMSO-d_6 at 313 K

Residue	HN	HN'	$^{\alpha}$CH	$^{\beta_1}$CH	$^{\beta_2}$CH	$^{\beta_3}$CH	$^{\gamma_1}$CH	$^{\gamma_2}$CH	$^{\gamma_3}$CH	$^{\delta}$CH
β-Ala-OBn	5.94	-	2.45	3.09 3.21	-	-	-	-	-	-
Res. 1	6.00	5.66	-	3.85	1.69	1.59	2.05 1.19	1.52	1.52	1.52
Res.2	5.71	6.29	3.26 2.20	3.66	-	-	0.79	-	-	-
Res. 3	6.06	5.46	-	4.15	1.68 2.48	1.76	1.24 1.96	1.51	1.51	1.51
Res. 4	5.88	6.51	2.36 3.48	-	-	-	2.60 2.51	-	-	-
Res. 5	6.18	5.63	-	4.19	1.68 2.39		1.21 1.95	1.51	1.51	1.51
Res. 6	6.16	6.15	2.84 3.19	3.66	-	-	0.97	-	-	-
4-BrPh	8.63	-	-	-	-	-	-	-	-	-

Oligourea 4

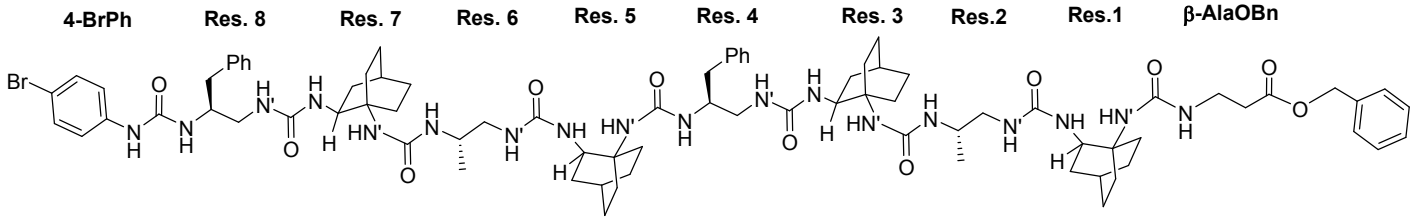

NMR chemical shifts for **4** could not be assigned in CD_3OH due to solubility issues.

Table S7. ^{1}H NMR chemical shifts for **4** in DMSO-d_6 at 298 K

Residue	HN	HN'	$^{\alpha}$CH	$^{\beta_1}$CH	$^{\beta_2}$CH	$^{\beta_3}$CH	$^{\gamma_1}$CH	$^{\gamma_2}$CH	$^{\gamma_3}$CH	$^{\delta}$CH
β-Ala-OBn	6.00	-	2.45	3.09 3.21	-	-	-	-	-	-
Res. 1	6.02	5.70	-	3.89	-	-	1.19 2.05	-	-	1.53
Res. 2	5.71	6.42	2.21 3.33	3.69	-	-	0.81	-	-	-
Res. 3	5.91	5.60	-	4.20	-	-	1.26 1.94	-	-	1.54
Res. 4	6.35	6.80	2.16 3.60	3.79	-	-	2.48 2.68	-	-	-
Res. 5	6.17	5.70	-	4.28	-	-	1.98 1.27	-	-	1.59
Res. 6	5.75	6.60	2.12 3.33	3.35	-	-	0.62	-	-	
Res. 7	6.29	5.60	-	4.28	-	-	1.25 1.98	-	-	1.59
Res. 8	6.29	6.22	2.98 3.32	3.93	-	-	2.72	-	-	-
4-BrPh	8.72	-	-	-	-	-	-	-	-	-

Table S8. Comparison of the ^{3}J(NH,$^{\alpha}$CH) et ^{3}J(NH,$^{\beta}$CH) coupling constants of oligourea hexamers in CD_3OH and DMSO-d_6.

^{3}J values between 8 and 10 Hz for the oligourea **3** were typical of antiperiplanar arrangements and shared close values to those measured for the [(*S*)-BAC]$_6$ and [(*R*)-BAC/(*S*)-AAC]$_3$ oligourea 12/14 helices. They were comparable in CD_3OH and DMSO-d_6. In contrast, the unfolded homochiral [(*S*)-BAC/(*S*)-AAC]$_3$ oligourea exhibited ^{3}J values < 8 Hz.[10]

Oligoureas/Solvents		Res.1	Res.2	Res.3	Res.4	Res.5	Res.6
3	^{3}J(NH,$^{\alpha}$CH)	8.3 Hz		9.8 Hz		9.9 Hz	
CD_3OH	^{3}J(NH,$^{\beta}$CH)		10.0 Hz		9.9 Hz		9.1 Hz
3	^{3}J(NH,$^{\alpha}$CH)	8.6 Hz		10.3 Hz		9.8 Hz	
DMSO-d_6	^{3}J(NH,$^{\beta}$CH)		9.4 Hz		9.6 Hz		9.5 Hz
[(*S*)-BAC]$_6$ CD_3OH	^{3}J(NH,$^{\alpha}$CH)	10.5 Hz	9.4 Hz	9.9 Hz	*nd*	9.9 Hz	8.0 Hz
[(*R*)-BAC/(*S*)-AAC]$_3$	^{3}J(NH,$^{\alpha}$CH)	9.7 Hz		10.4 Hz		10.3 Hz	
CD_3OH	^{3}J(NH,$^{\beta}$CH)		9.8 Hz		9.2 Hz		8.7 Hz
[(*R*)-BAC/(*S*)-AAC]$_3$	^{3}J(NH,$^{\alpha}$CH)	9.0 Hz		9.9 Hz		9.2 Hz	
DMSO-d_6	^{3}J(NH,$^{\beta}$CH)		8.9 Hz		9.6 Hz		*nd*
[(*S*)-BAC/(*S*)-AAC]$_3$	^{3}J(NH,$^{\alpha}$CH)	7.6 Hz		7.4 Hz		*nd*	
DMSO-d_6	^{3}J(NH,$^{\beta}$CH)		7.5 Hz		*nd*		7.5 Hz

nd: not determined due to signal overlaps. The [(S)-BAC]$_6$ oligomer was not studied in DMSO-d_6.[9] *Broad linewidths in CD_3OH prevent the ^{3}J accurate measurements for [(S)-BAC/(S)-AAC]$_3$.*[10]

Table S9. Comparison of the chemical shift differences Δδ (in ppm) of the $^{\alpha}CH_2$ protons of the acyclic residues in hexamer sequences.

Noticeable chemical shift differences (Δδ(αCH) > 0.35 ppm, up to 1.27 ppm) were observed between the diastereotopic αCH protons of the acyclic motifs for the helical oligourea **3** and (*R*)-BAC/(*S*)-AAC hexamer. In contrast, the αCH methylene pairs were degenerated (Δδ(αCH) < 0.11 ppm) for the (*S*)-BAC/(*S*)-AAC and thus shared a similar environment.

oligoureas	Solvent	APC (Res. 2)	APPC (Res. 4)	APC (Res. 6)
3	CD_3OH	1.02	1.27	0.89
	DMSO-d_6	1.06	1.12	0.35
(*R*)-BAC/(*S*)-AAC	CD_3OH	1.21	1.28	1.05
	DMSO-d_6	0.89	1.17	0.7
(*S*)-BAC/(*S*)-AAC	CD_3OH	0.07	0.08	0.1
	DMSO-d_6	0.09	0.11	0

It is worth noting that the analysis of the ^{3}J values and Δδ(αCH_2) values of the acyclic residues are indicative of the global fold and stability of the oligoureas but do not account for slight local distortions or bias.

Figure S8. ^{1}H NMR spectra of **1** (in purple), **2** (in green), **3** (in red) and **4** (in blue) in CD_3OH at 313 K.

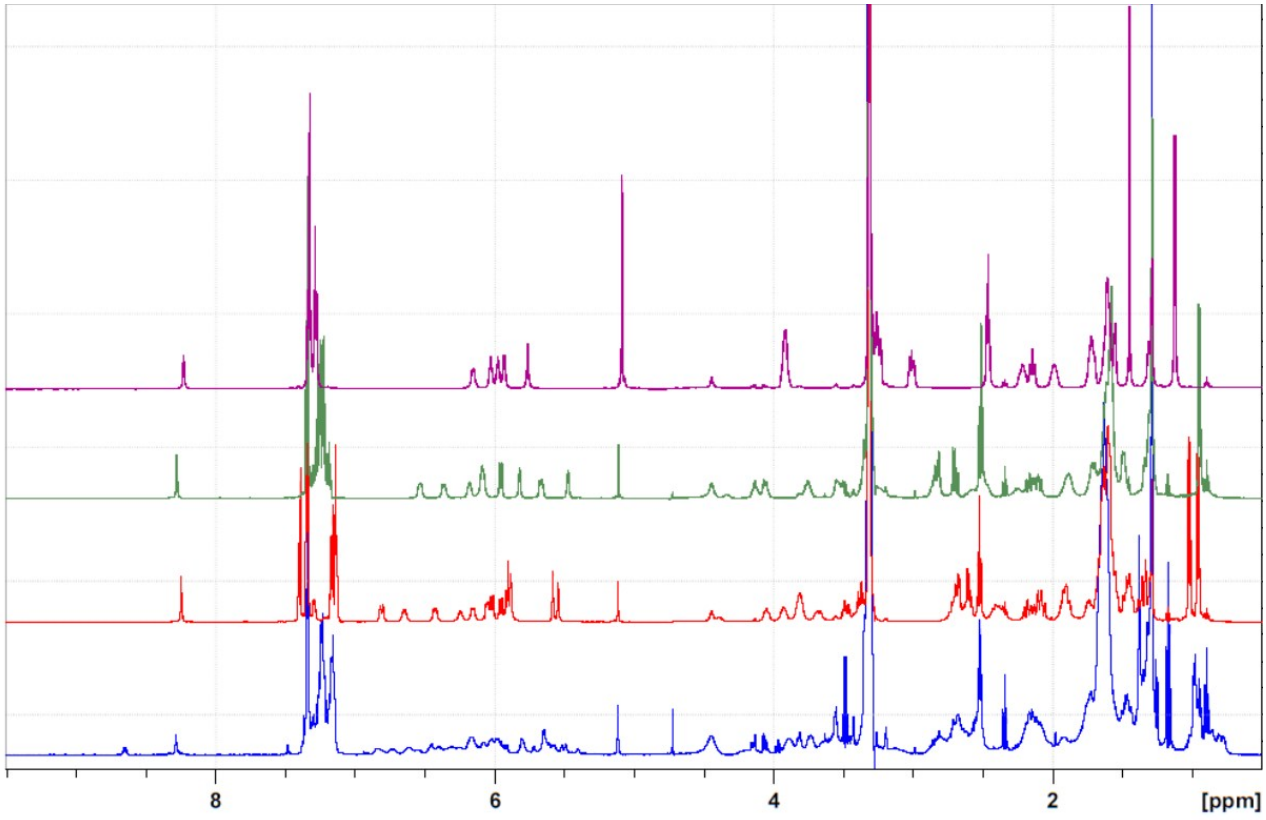

Figure S9. ROESY spectrum of **1** in CD_3OH at 313 K.

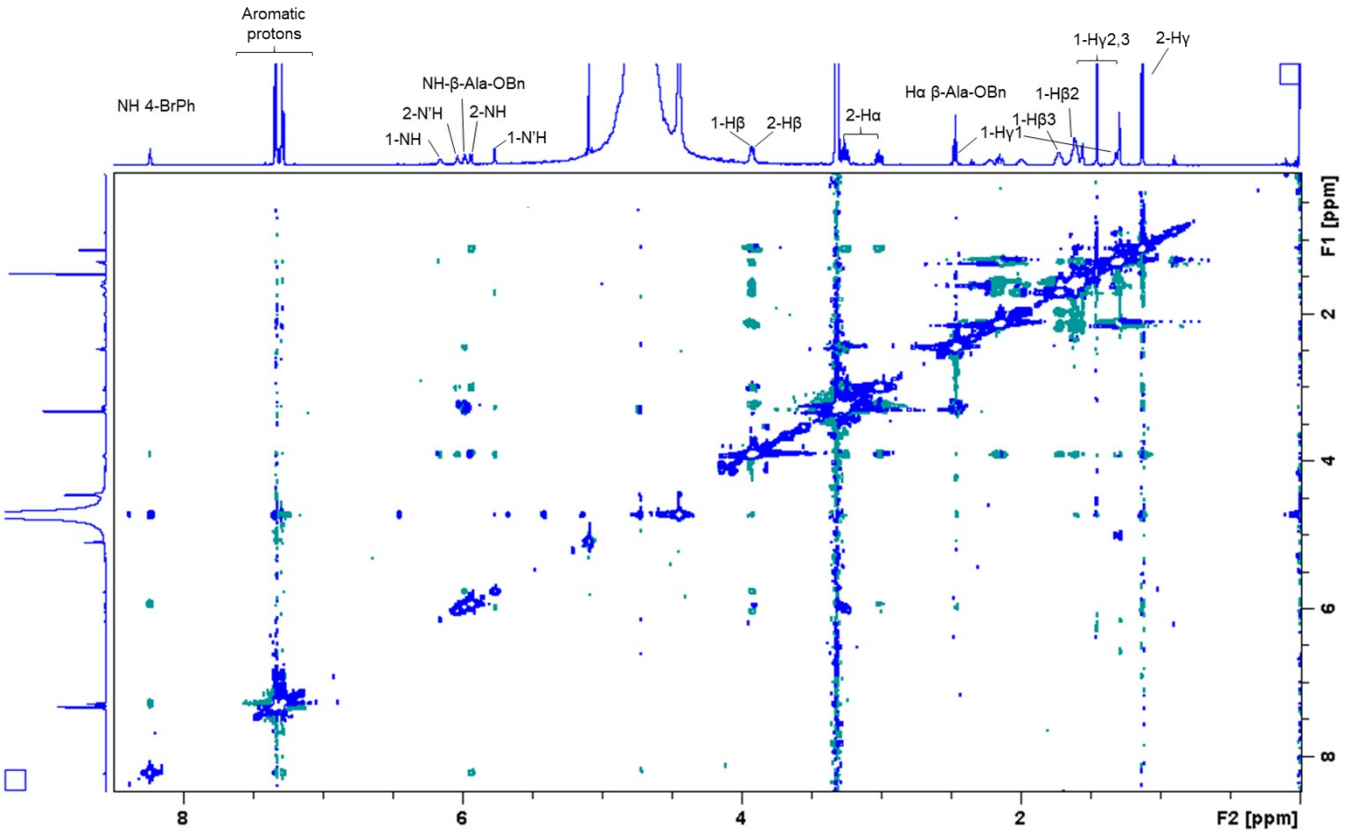

Figure S10. ROESY spectrum of **2** in CD_3OH at 298 K.

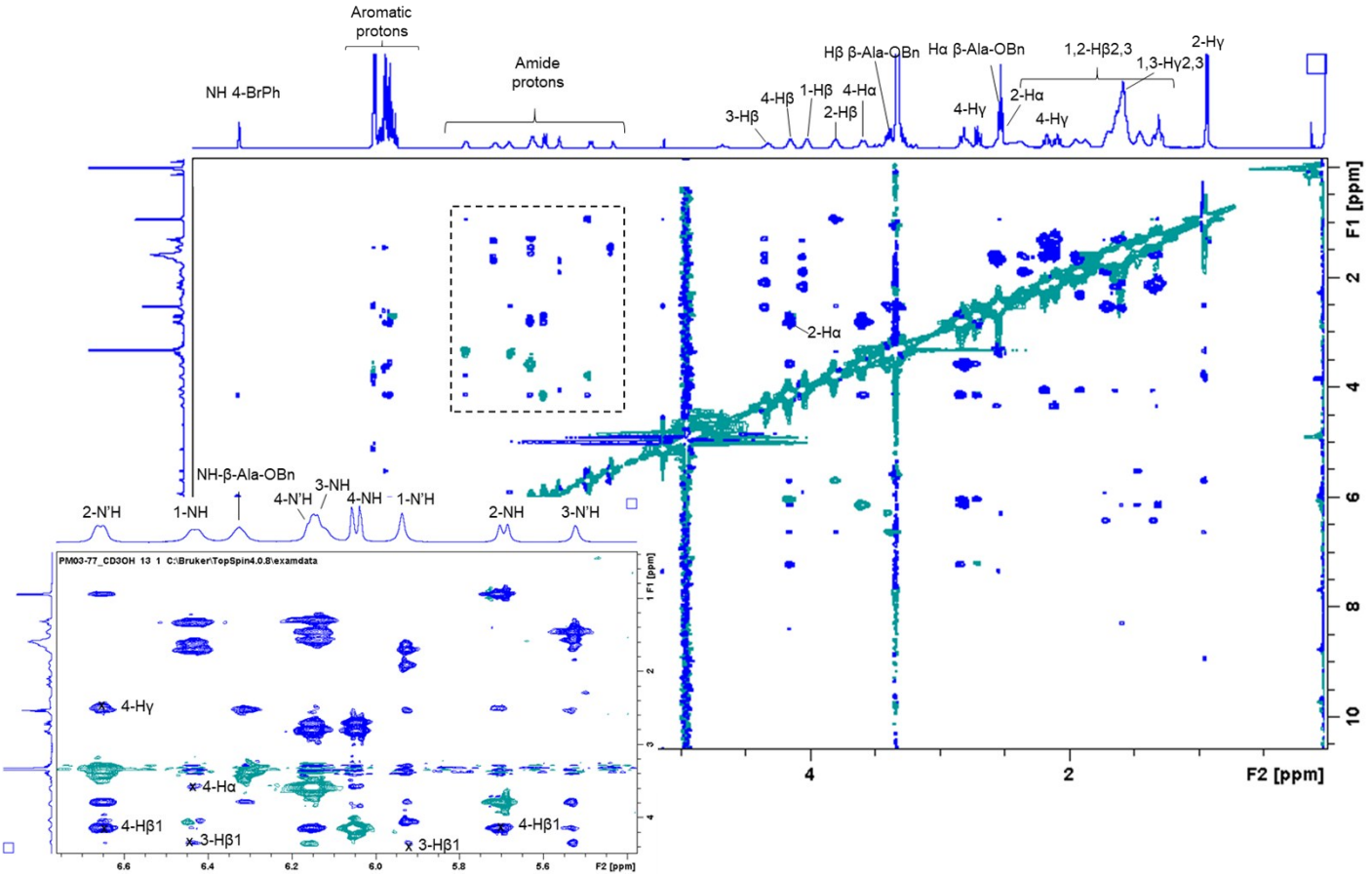

Figure S11. ROESY spectrum of **3** in CD_3OH at 298 K.

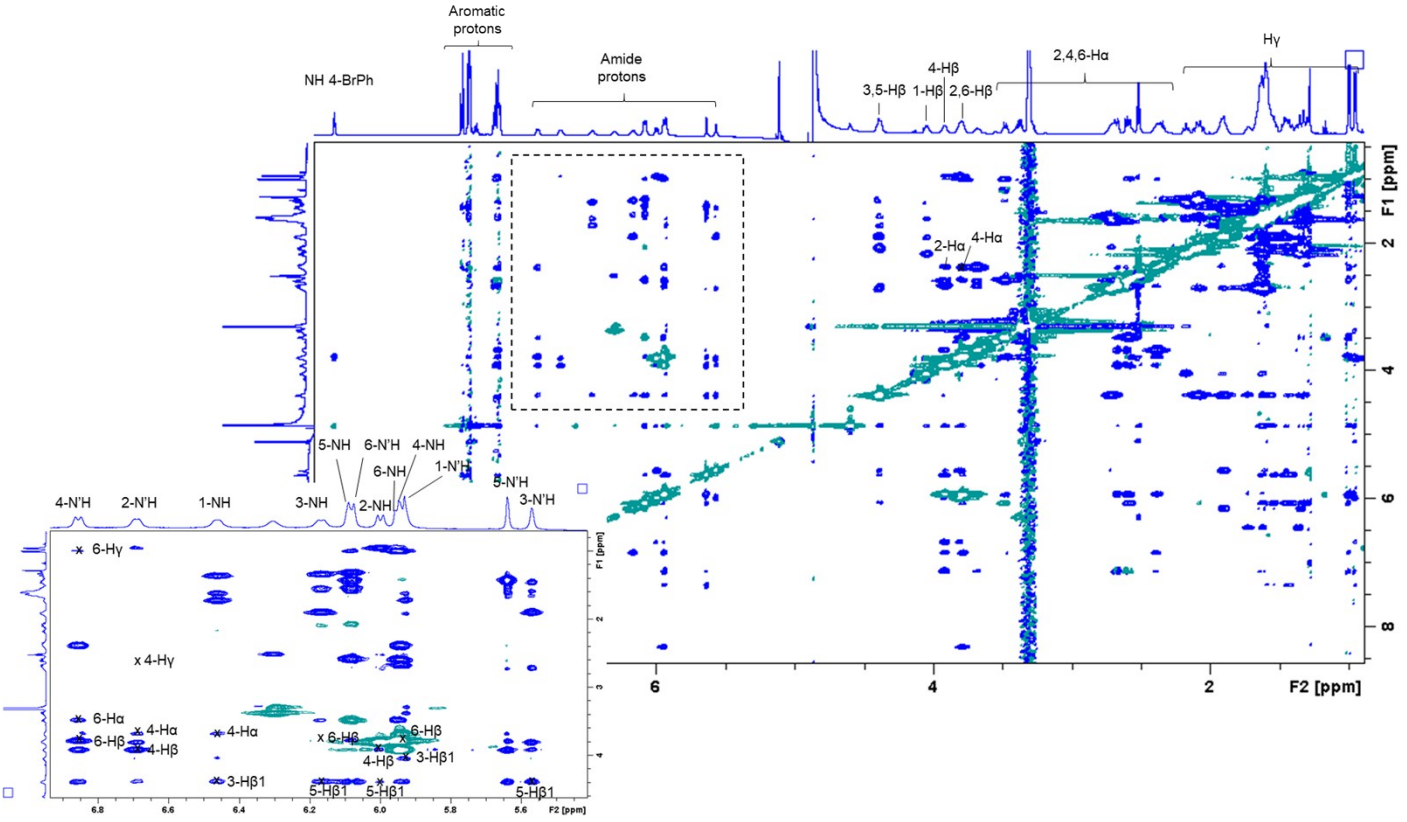

Figure S12. ^{1}H NMR spectra of **1** (in purple), **2** (in green), **3** (in red) and **4** (in blue) in DMSO-d_6 at 298 K.

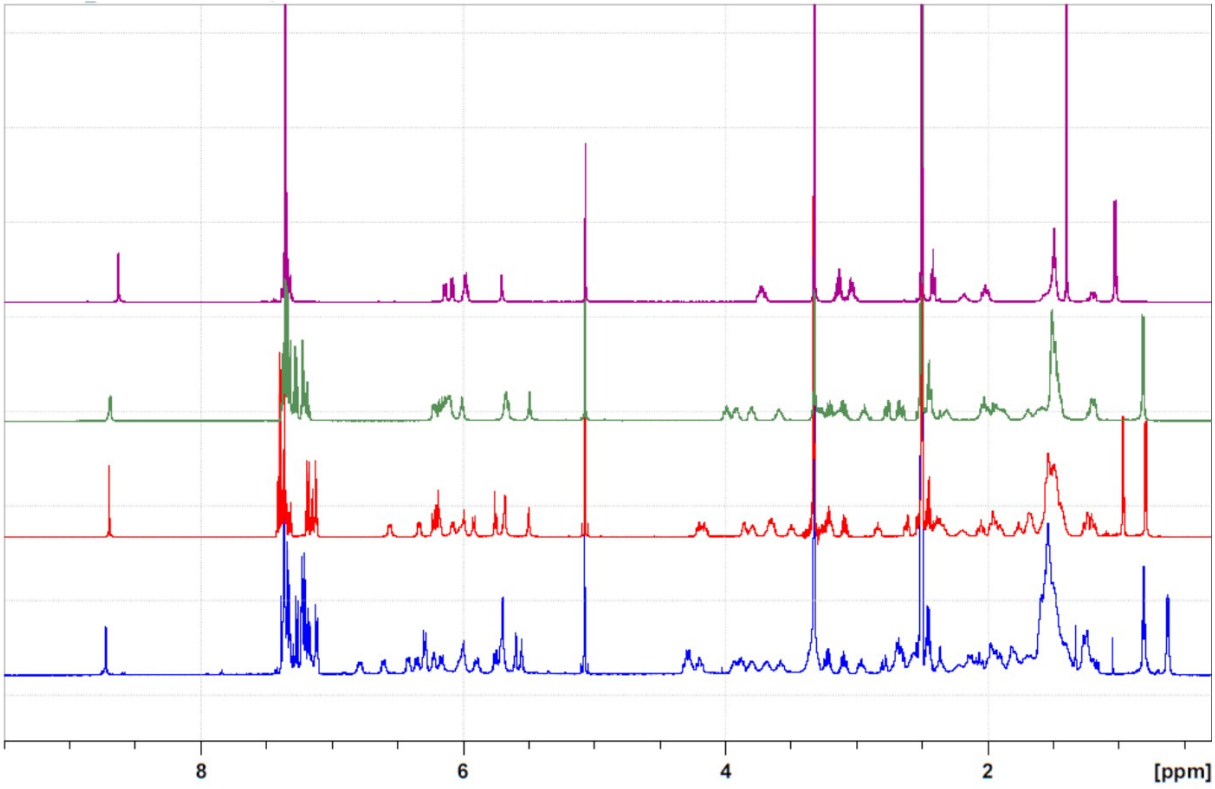

Figure S13. ROESY spectrum of **1** in DMSO-d_6 at 298 K.

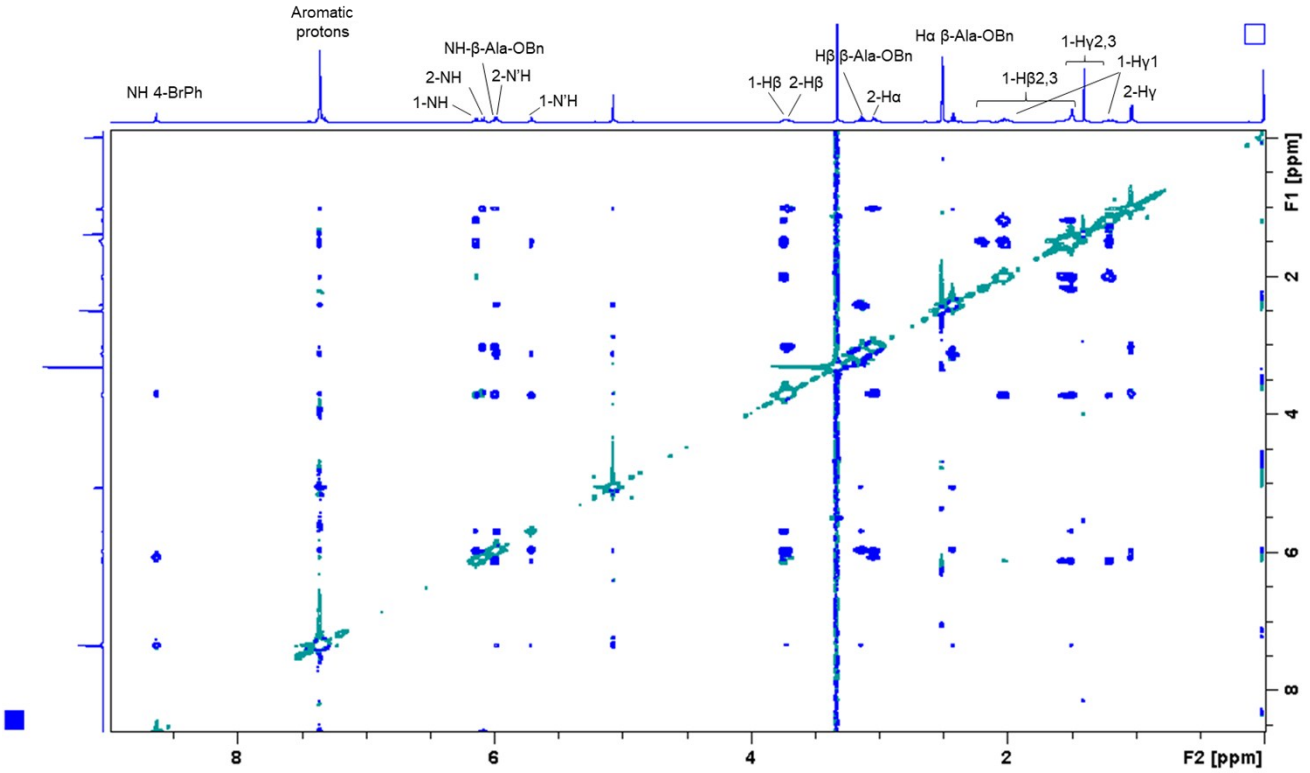

Figure S14. ROESY spectrum of **2** in DMSO-d_6 at 298 K.

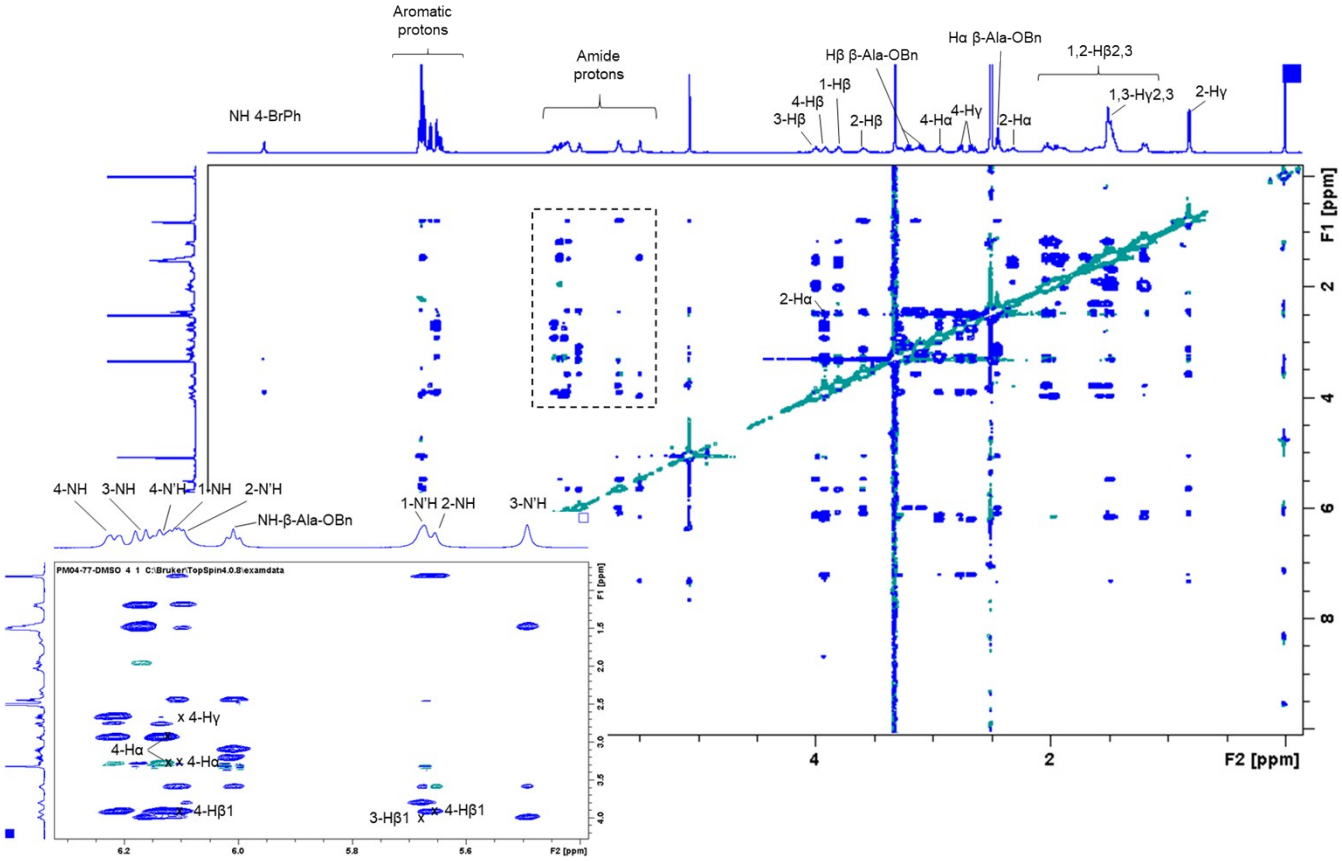

Figure S15. ROESY spectrum of **3** in DMSO-d_6 at 313 K.

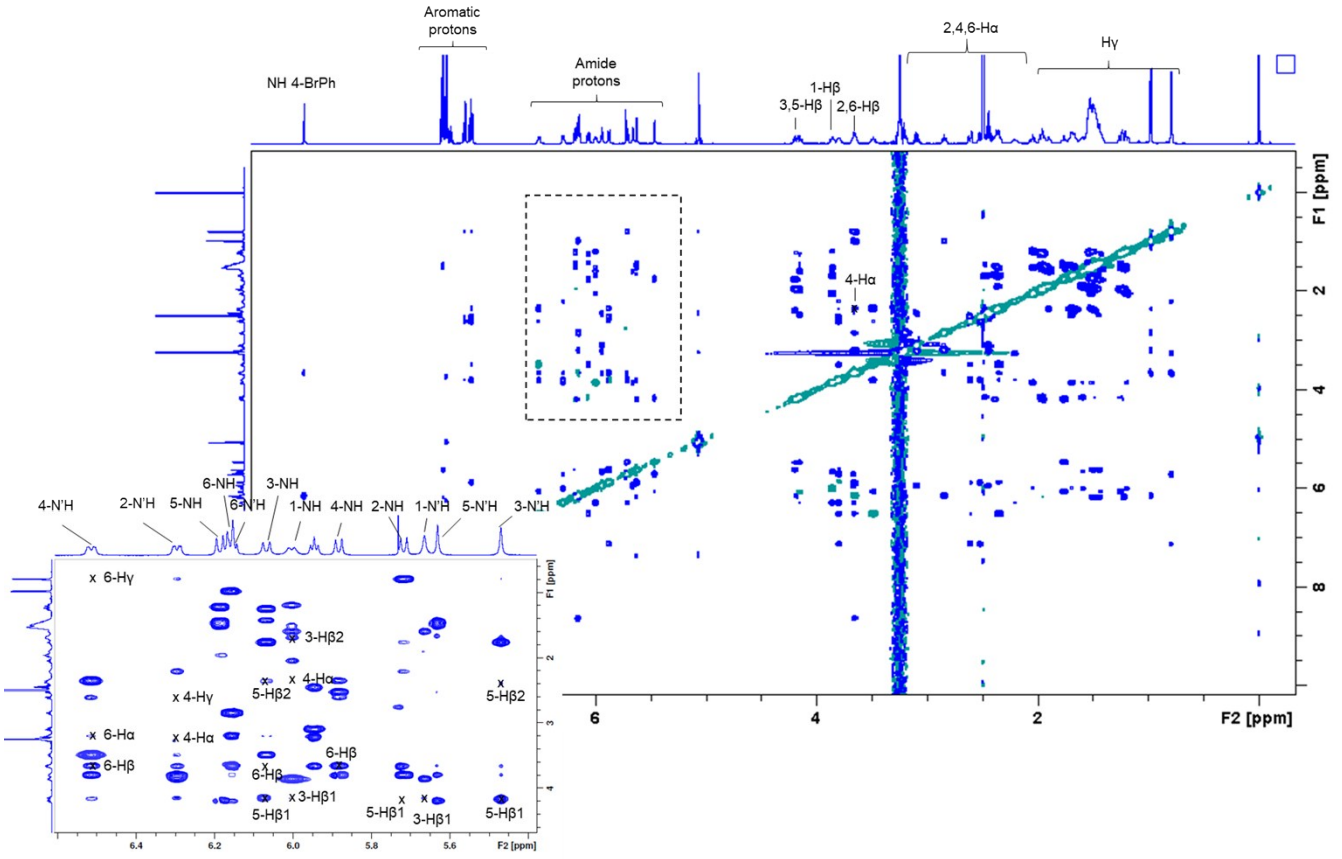

Figure S16. ROESY spectrum of **4** in DMSO-d_6 at 313 K

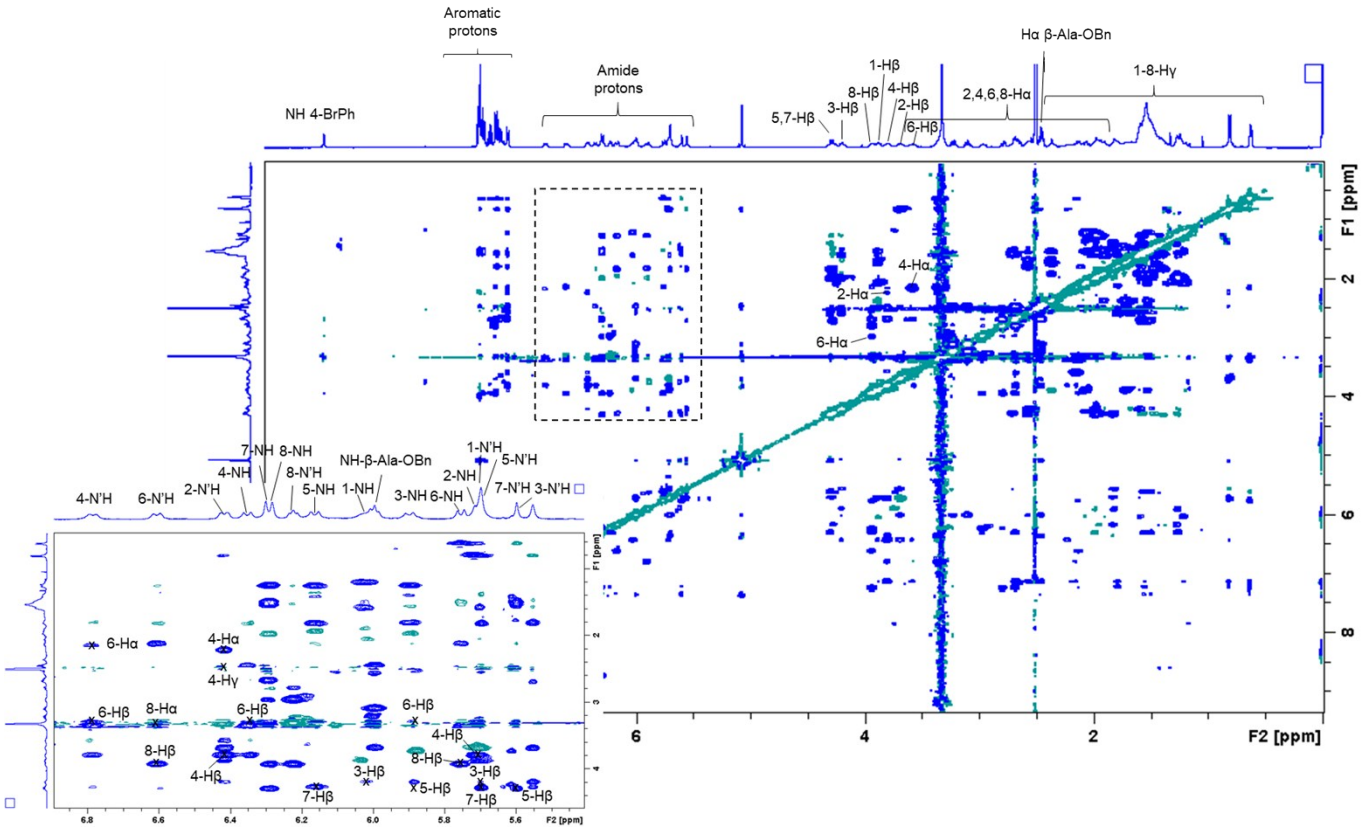

Crystallographic data

X-ray data were collected at 100K with a Rigaku Oxford Diffraction SuperNova diffractometer using Mo-Kα and Cu-Kα microsources for the tetramer **2** and octamer **4**, respectively. Diffraction data were processed using CrysAlis RED.[a]

All structures were solved using the dual-space algorithm of SHELXT, and the crystallographic refinements were conducted using SHELXL-97.[b] Olex2 was used as an interface to all SHELX programs, and to prepare material for publication.[c] The solvent contribution to the structure factors was taken into account for the tetramer **2** using a solvent mask in Olex2.[c] All hydrogen atoms were inserted at calculated positions, and refined using a riding model. Their isotropic thermal displacement parameters were fixed at 1.2×Ueq (or 1.5×Ueq) of the parent atom to which they were attached. Selected crystallographic data are provided in the table S1.

CCDC 1982733, and CCDC 1982734 contain the supplementary crystallographic data for this paper. These data can be obtained free of charge from The Cambridge Crystallographic Data Centre via www.ccdc.cam.ac.uk/data_request/cif

(a) Oxford Diffraction, 2003.
(b) G. M. Sheldrick, *Acta Crystallogr A Found Adv* 2015, **71**, 3-8.
(c) O. V. Dolomanov, L. J. Bourhis, R. J. Gildea, J. A. K. Howard and H. Puschmann, *Journal of Applied Crystallography* 2009, **42**, 339-341.

T**able S10.** Selected Crystallographic data for the oligoureas **2** and **4**

Oligoureas	**2**	**4**
Formula	$C_{49}H_{65}BrN_{10}O_7$	$C_{81}H_{113}BrN_{18}O_{11}$
Space group	*P*1	$P4_3$
a	10.0071	11.7593
b	10.6965	11.7593
c	12.3292	63.070
alpha	90.333	90
beta	103.664	90
gamma	108.641	90
Volume	1210.35	8721.4
Z'	1	1
Nref (measured)	56632	42420
R_{int}	0.040	0.064
Completeness	1.0	0.997
d_{max} (Å)	0.711	0.792
R_1 ($F^2 > 2\sigma(F^2)$)	0.0383	0.986
wR_2 (all data)	0.0895	0.2471
S ($F^2 > 2\sigma(F^2)$)	1.062	1.080
N_{par}	605	1002

Figure S17. ORTEP view of oligourea **2**. Thermal ellipsoids are drawn at 50 % probability. Hydrogen atoms, except for nitrogen atoms and the asymmetric carbon atom, have been omitted for clarity.

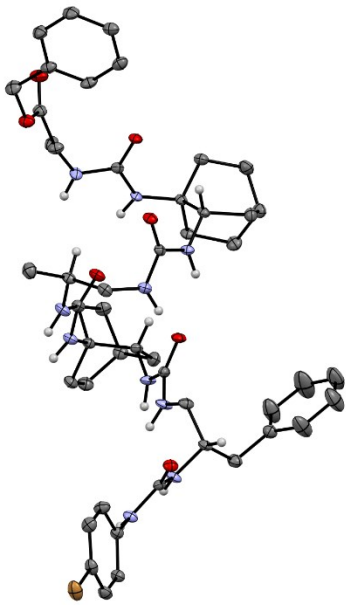

Figure S18. ORTEP view of oligourea **4**. Thermal ellipsoids are drawn at 50 % probability. Hydrogen atoms, except for nitrogen atoms and the asymmetric carbon atom, have been omitted for clarity.

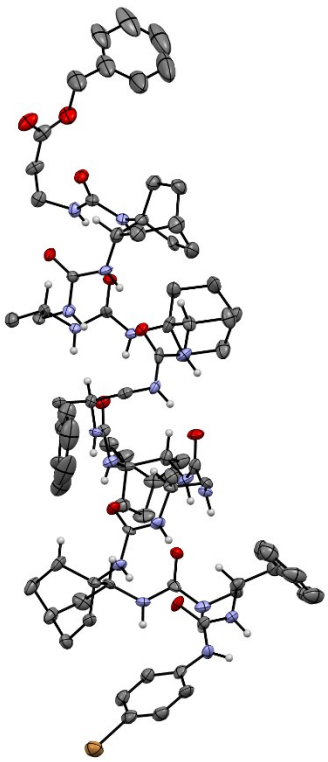

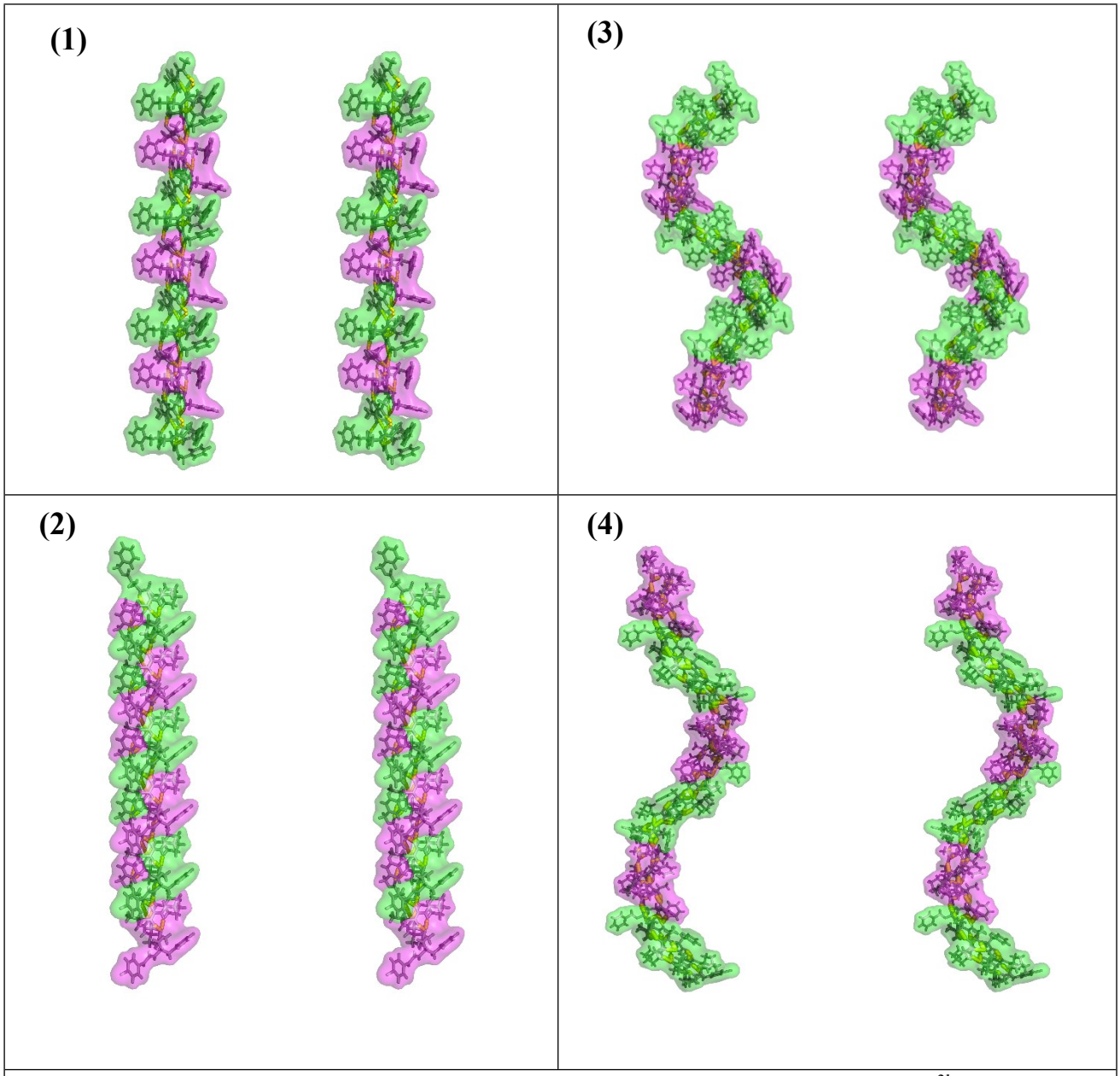

Figure S19. Stereo views of the linear stacking of the tetramers Homo-[(*S*)-AAC]$_4^{3h}$ (1) and **2** (2) and the helical stacking of the octamers Homo-[(*S*)-AAC]$_8^{3h}$ (3) and **4** (4). Oligomers are shown in stick representation. Their van der Waals surfaces are displayed in green of magenta transparency. Intra and Intermolecular hydrogen bonds are shown in yellow dashed sticks. In the crystal of **2** the molecules form straight helical columns, while in the crystal of **4**, the molecules are not aligned. The axes of two consecutive helices are deviated from ca 60° and the molecules generate H-bonded left-handed super-helices in the $P4_3$ space group.

DFT calculations

Gas-phase calculations: Based on the structural data gathered on the BAC and *r*BAC oligoureas, four models of (*S*)-BAC/(*S*)-AAC and (*S*)-*r*BAC/(*S*)-AAC mixed oligourea hexamers were build and optimized at the density functional level of theory using the Gaussian 09 software[a] (see below, Fig. S17).

Figure S20. (1) Oligourea hexamers used for the DFT calculations. (2) Backbone torsion angle values of the initial 12/14-helix structures (in °). They are average values measured on the crystal structures of **2** and **4**.

(1)

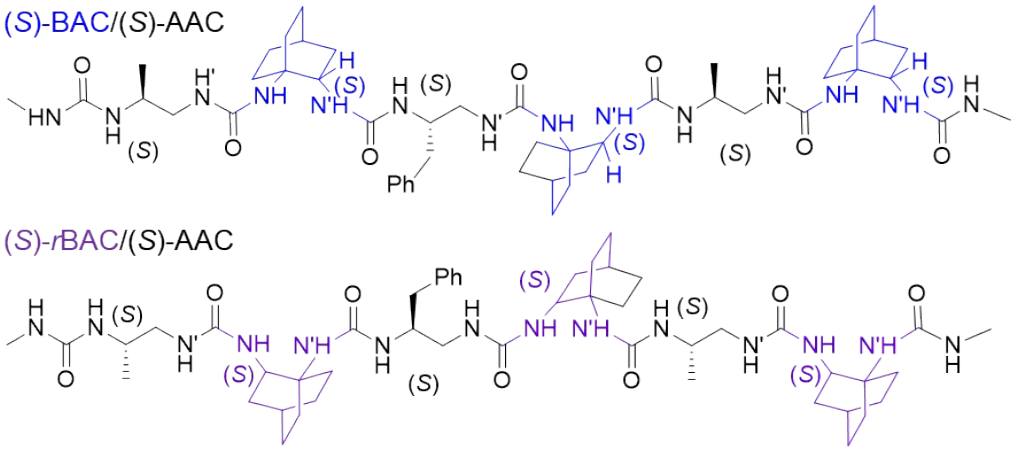

(2)

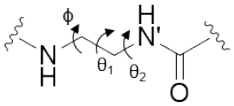

Residues	Angles	(*S*)-BAC/(*S*)-AAC	(*S*)-*r*BAC/(*S*)-AAC
BAC/rBAC	θ_2	-97	68
	θ_1	54	54
	ϕ	68	-97
AAC (APC/APPC)	θ_2	-105	84
	θ_1	56	56
	ϕ	84	-105
Handedness		Right	Right

To reduce the computational cost, acetyl groups substituted the N- and C-terminal cappings. The B3LYP functional[b] was used along with the 6-31(d,p) basis set. Empirical dispersion was taken into account through Grimme's D3 damping function[c]. No solvent effect was considered (calculation in vaccum) and frequency calculation was performed to check that an energy minimum was obtained at the end of the optimization procedure.

Figure S21: (1) Optimized 12/14-helix structures at the B3LYP-D3/6-31G(d,p) level of theory. (2) Average backbone torsion angle values in the optimized structures (in °).

(1)

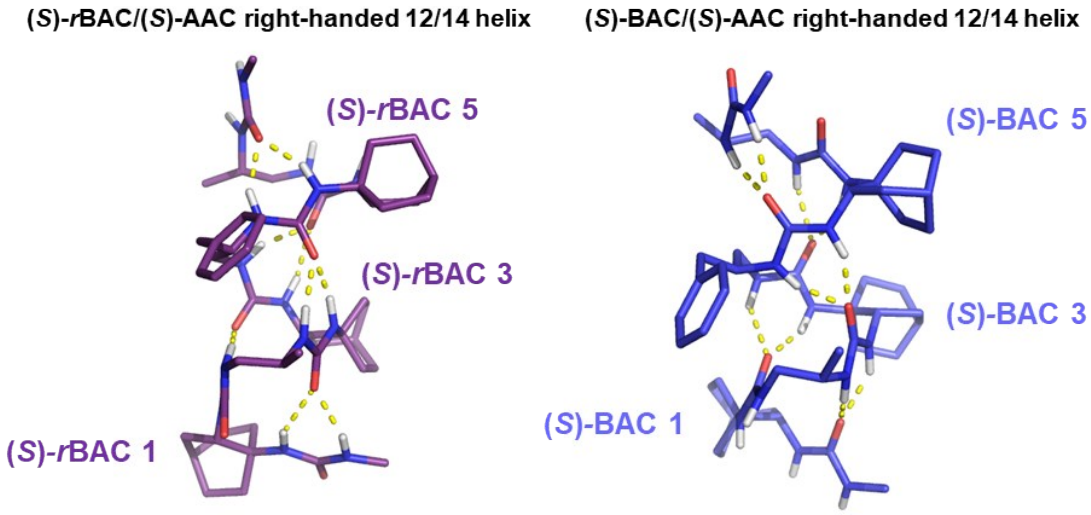

(2)

Residues	Angles	(*S*)-BAC/(*S*)-AAC	(*S*)-*r*BAC/(*S*)-AAC
BAC/rBAC	θ_2	-103 ± 14	64 ± 4
	θ_1	60 ± 1	55 ± 7
	ϕ	66 ± 6	-103 ± 11
AAC (APC/APPC)	θ_2	-96 ± 4	78 ± 6
	θ_1	65 ± 9	57 ± 4
	ϕ	72 ± 1	-108 ± 14
Handedness		Right	Right

Table S11: Energy differences between the homochiral oligoureas 12/14-helices.

Oligoureas	B3LYP-D3/6-31G(d,p) (a.u.)	ΔG (kJ.mol^{-1})
(*S*)-BAC/(*S*)-AAC	-3168.612137	31.05
(*S*)-*r*BAC/(*S*)-AAC	-3168.623973	0.00

(a) Gaussian 09. Revision C.01, Frisch, M. J.; Trucks, G. W.; Schlegel,H. B.; Scuseria, G. E.; Robb, M.; Cheeseman, J. R.; Scalmani, G.;Barone, V.; Mennucci, B.; Petersson, G. A.; Nakatsuji, H.; Caricato,M.; Li, X.; Hratchian, H. P.; Izmaylov, A. F.; Bloino, J.; Zheng, G.;Sonnenberg, J. L.; Hada, M.; Ehara, M.; Toyota, K.; Fukuda, R.;Hasegawa, J.; Ishida, M.; Nakajima, T.; Honda, Y.; Kitao, O.;Nakai, H.; Vreven, T.; Montgomery, Jr. J. A.; Peralta, J. E.; Ogliaro,F.; Bearpark, M.; Heyd, J. J.; Brothers, E.; Kudin, K. N.; Staroverov,V. N.; Keith, T.; Kobayashi, R.; Normand, J.; Raghavachari, K.;Rendell, A.; Burant, J. C.; Iyengar, S. S.; Tomasi, J.; Cossi, M.; Rega, N.; Millam, J. M.; Klene, M.; Knox, J. E.; Cross, J. B.;Bakken, V.; Adamo, C.; Jaramillo, J.; Gomperts, R.; Stratmann,R. E.; Yazyev, O.; Austin, A. J.; Cammi, R.; Pomelli, C.; Ochterski,J. W.; Martin, R. L.; Morokuma, K.; Zakrzewski, V. G.; Voth, G. A.;Salvador, P.; Dannenberg, J. J.; Dapprich, S.; Daniels, A. D.; Farkas,O.; Foresman, J. B.; Ortiz, J. V.; Cioslowski, J. and Fox, D. J.: Gaussi-an, Inc., Wallingford CT,2010

(b) A. D. Becke, J. Chem. Phys.1993,98, 5648–5652

(c) S. Grimme, J. Antony, S. Ehrlich and H. Krieg, J. Chem. Phys., 2010, 132, 154104.

One could logically suspect detrimental bicyclic-bicyclic interactions as the primary cause of destabilization and thus, it could be interesting to have a close look at the BAC/rBAC relative positions in their respective 12/14-helix. We measured short but comparable bicyclic-bicyclic minimal average distances, e.g. $d_{H\text{-}H}$= 2.0 ± 0.1 Å and 2.2 ± 0.1 Å in the (*S*)-BAC/(*S*)-AAC and (*S*)-rBAC/(*S*)-AAC helices, respectively. The successive bicyclic residues are periodically shifted of ca 60° in both helices, which may minimize detrimental strong inter-bicyclic steric clashes. The largest difference between both structures relies in the urea bond direction and the AAC side chains projection (Fig. 3b and S21), causing notable backbone-side chain steric clashes. We hypothesized that such interactions mainly prevented the folding of the (*S*)-BAC/(*S*)-AAC oligomer.